REPORT No. 774

EFFECT OF TILT OF THE PROPELLER AXIS ON THE LONGITUDINAL-STABILITY CHARACTERISTICS OF SINGLE-ENGINE AIRPLANES

By Harry J. Goett and Noel K. Delany

SUMMARY

The results of tests of a model of a single-engine airplane with two different tilts of the propeller axis are reported herein. The results indicate that on a typical design a 5° downward tilt of the propeller axis will considerably reduce the destabilizing effects of power. This reduction is equivalent to as much as a 0.05 mean aerodynamic chord favorable shift of the neutral point for 2,100-horsepower operation (at a C_L of 0.8). For 3,450-horsepower operation the increase in the stability is equivalent to a 0.10 M. A. C. shift in the stick-fixed neutral point at a C_L of 0.8. The improvement in handling characteristics (elevator angle and stick force against velocity, and stick force against normal acceleration) resulting from these effects is evaluated. It is shown that, by use of the tilted propeller, the stick force in accelerated maneuvers can be reduced at no sacrifice of power-on stability.

A comparison of the experimental results with those computed by use of existing theory is included. It is shown that the results can be predicted with an accuracy acceptable for preliminary design purposes, particularly at the higher powers where the effects are of significant magnitude.

INTRODUCTION

The designer of a modern pursuit airplane is confronted with the conflicting requirements of maneuverability and stability and, due to the large effects of power, it is becoming progressively more difficult to compromise these requirements in a single-engine airplane. For example, present flying qualities specifications call for a low stick force per unit normal acceleration and, at the same time, require stick-fixed and stick-free stability under flight conditions where the effects of power are large (e. g., a rated-power climb or partial-power approach). A low longitudinal stability is conductive to the attainment of the former requirement, while a high stability (with power off or at high speed) is required by the latter. The margin necessary on a modern single-engine fighter tends to be so great that in order to attain the desired light stick force in maneuvers, an unduly close-balanced elevator must be resorted to.

As an illustration of this point, consider a typical single-engine airplane powered with a 2,100-horsepower engine, weighing 14,000 pounds, and with a wing loading of 40 pounds per square foot. With an airplane of normal dimensions a forward shift of the neutral point of as much as 10 percent M. A. C. will occur, due to the application of rated power at a C_L of 0.8 (143 mph). If stability is to be maintained in this condition, a dC_m/dC_L of at least -0.10 must exist power off (or at high speed where the effects of power are small). If the stick force in steady turns is to be kept within the limit of 8 pounds per g (which is required for a fighter or an attack airplane), a $dC_h/d\delta_e$ of the order of -0.001 on a 30-percent-chord elevator is required. The maintenance of this close balance over anything but a limited elevator-deflection range will be difficult, and the control will be subject to overbalance due to small manufacturing deviations in contour or due to Mach number effects.

It is apparent that any design change in the airplane, which will reduce the destabilizing effects of power, will permit the reduction of the power-off stability which must be built into the airplane. Thus, the attainment of *both* a low stick force per g and stability in high-powered low-speed flight will be facilitated. An effective means for decreasing the destabilizing effects of power is to give the propeller thrust axis a slight downward tilt. A 5° tilt on an airplane of normal nose length will give the thrust axis a moment arm of the order of 0.1 M. A. C. about the center of gravity. On the typical airplane being considered, the resulting thrust moment (if fully effective) would cause a stabilizing increment of -0.04 in dC_m/dC_L at a C_L of 0.8 for climb with 2100 horsepower (T_c=0.27). The schematic sketch on figure 1 shows that a tilt of this magnitude could be attained with very little, if any, change in the external lines of the airplane.

In addition to the effect of tilt of the propeller arising directly from the propeller forces, there will be a secondary effect on the slipstream which also will be beneficial. Since the vertical component of the thrust is decreased by tilting the thrust axis downward, the change in downwash resulting from this vertical component will also be decreased.[1] The stabilizing effect of the decreased change in downwash cannot be computed readily, but rough estimates indicate that it could be about half as large as the effect due to thrust moment.

Thus, this cursory examination indicates that the forward shift of the neutral point might be reduced from about 0.10 M. A. C. with an untilted propeller axis to 0.04 M. A. C. with a 5° tilt (figures given for 2,100 hp. at a C_L of 0.8). However, there was the possibility that a given geometric tilt of the thrust axis might not result in an equal angular

[1] The destabilizing effects of power are traceable in a large measure to the increase of down wash in the slipstream and the resulting influence on the tail-pitching moment.

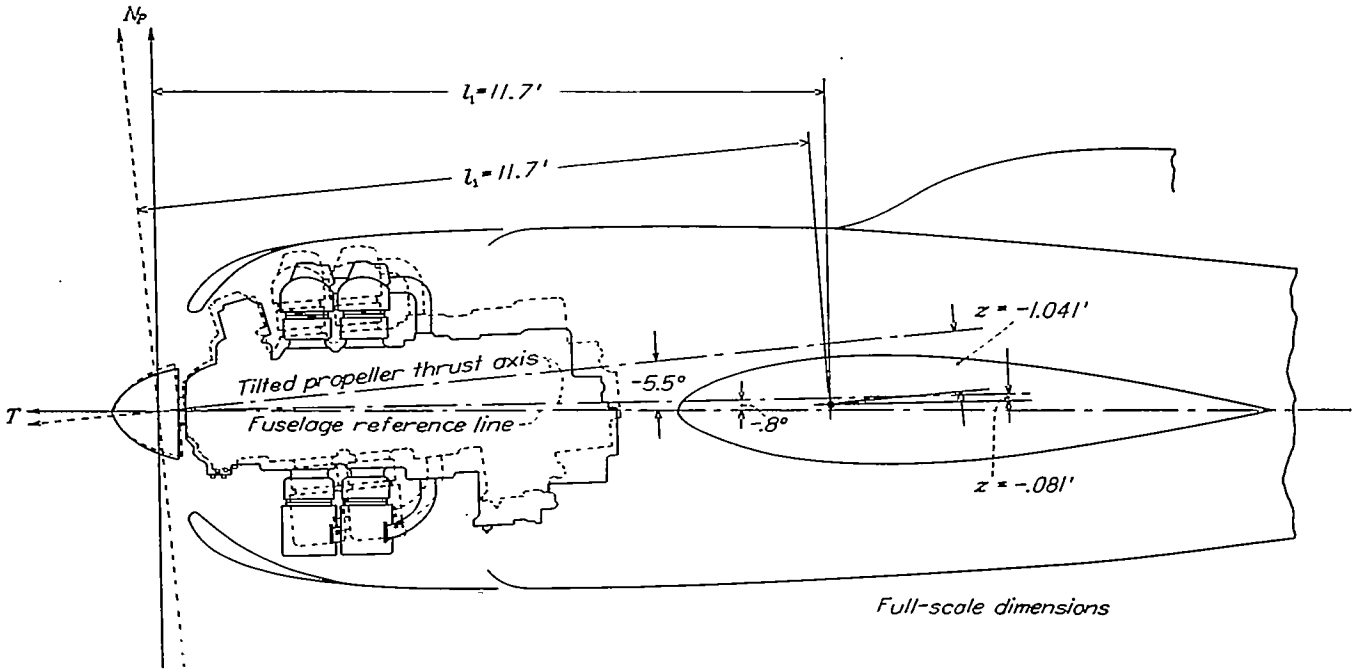

$$\Delta M_{prop} = Tz + N_p l_1$$

$$\Delta C_{m_{prop}} = \frac{Tz}{\frac{1}{2}\rho V^2 Sc} + \frac{N_p l_1}{\frac{1}{2}\rho V^2 Sc}$$

$$\Delta C_{m_{prop}} = T_c \frac{2D^2}{S}\frac{z}{c} + \frac{K \sin\theta}{(V/nD)^2}\frac{2D^2}{S}\frac{l_1}{c}$$

FIGURE 1.—Schematic installation of tilted engine.

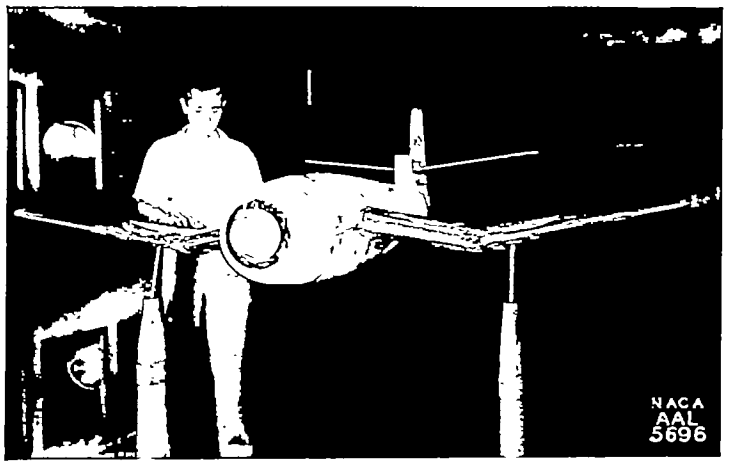

(a) Normal tail

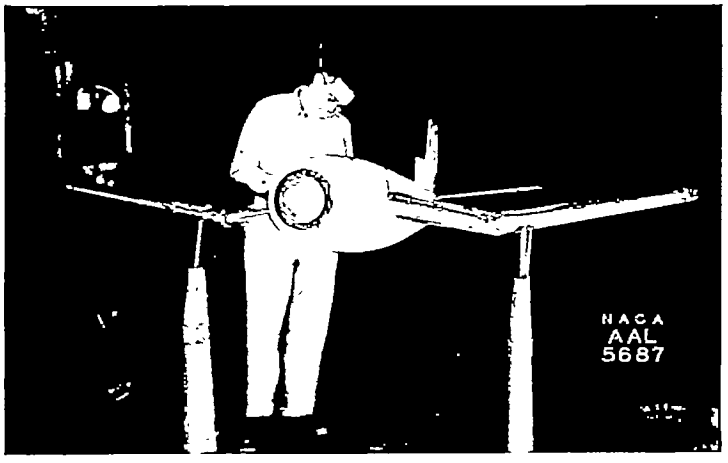

(b) Revised tail

FIGURE 2.—Single-engine airplane model mounted in the 7- by 10-foot tunnel

change of the line of action of the thrust. There also was a need for verification of the computed effects on the tail and a determination of the influence of the position of the tail with respect to the slipstream. Accordingly, the tests reported herein were conducted on a model of a typical single-engine airplane with two different tilts of the propeller axis. This report presents the results, shows the effects on the associated flying qualities, and compares the effects with those computed from the basic theory involved. The symbols used throughout the report are defined in appendix A.

MODEL AND APPARATUS

All tests were run in the Ames 7- by 10-foot wind tunnel No. 2. Figure 2 shows the model mounted in the tunnel.

A three-view drawing of the model is shown on figure 3. It was assumed to be a $\frac{3}{16}$-scale model of an airplane weighing 14,700 pounds, wing loading 39.2. The characteristic dimensions of the model and the full-scale airplane (assuming $\frac{3}{16}$ scale) are given in the table on figure 3. The model was equipped with vaned, slotted flaps. It will be noted that there are two tail locations: one designated the normal tail position, and the other the raised tail position. Figure 4 shows the location of these tails relative to the fuselage reference line (a line corresponding to an untilted thrust axis).

Unless specifically stated otherwise all pitching moments herein are referred to the 0.25 M. A. C. point, the location of which is shown on figure 3. The relation of the thrust axis, center of gravity, and wing is given in more detail in figure 1. Tilts of the propeller of −0.8° and −5.5° were tested. (Negative sign indicates a downward tilt.) This tilt was obtained by rotating the motor about a horizontal line passing

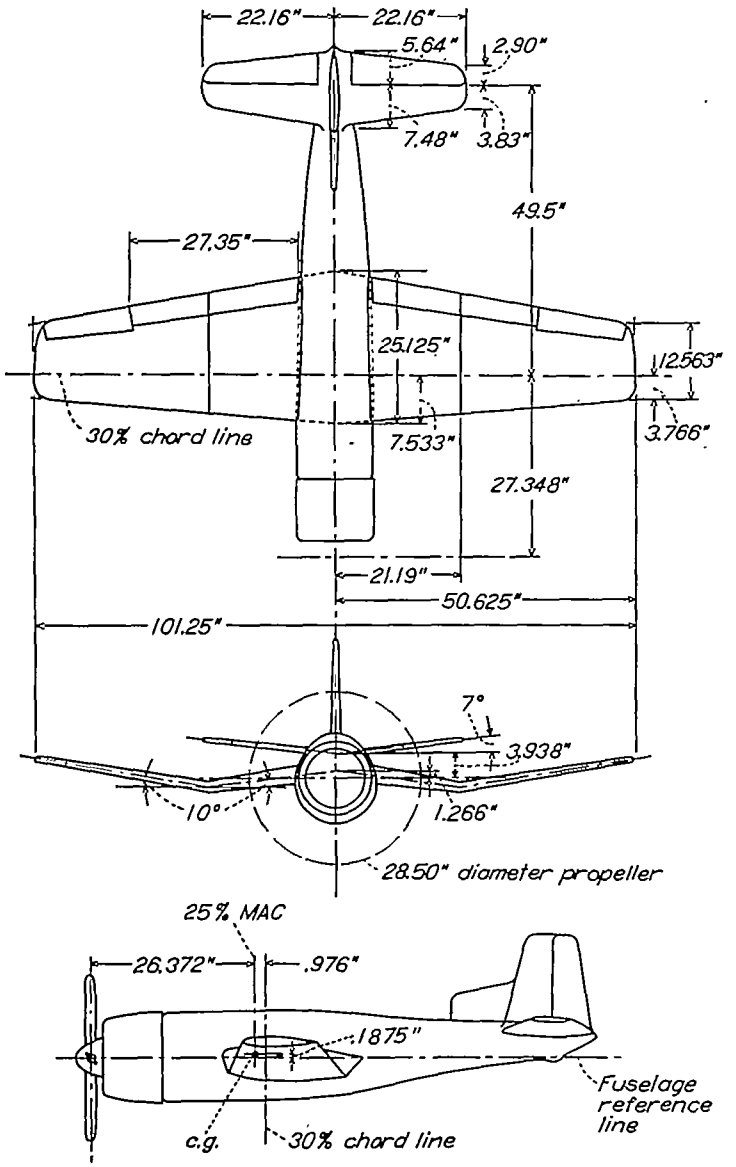

through the center of rotation of the propeller. Thus the vertical position of the propeller was not affected by the tilt. Sufficient clearance existed inside the cowl so that the motor could be tilted without any alteration of the external lines of the model.

Details of the horizontal tail surface are shown in figure 5. The tail volume was 0.535, which is believed to be in the normal range for this type of airplane. The elevator was restrained by an electrical-type strain gage which was used for the measurement of hinge moments. In the computation of stick forces from the hinge moments, a 32° movement of a 25.5-inch stick was assumed with the elevator operating in a deflection range of 20° to −30°. With a linear relation this gives an F/HM of 0.735.

The model was powered with a 100-horsepower motor driving a four-blade single-rotating propeller. All tests were run with the propeller set at a blade angle of 21.0° at the $0.75R$. The experimentally determined T_c against V/nD relationship for this setting is shown in figure 6. The variation of K (propeller normal-force factor) with V/nD as computed from the experimentally determined C_p against V/nD characteristics of the model propeller at a 21.0° blade

	Basic data	
	Full scale	Model scale
Gross weight	14,700 lbs	
Wing span	45 ft	8.36 ft.
Wing area	375 sq. ft	13.181 sq. ft.
MAC	8.7 ft	1.63 ft.
Aspect ratio	5.4	5.4.
Root chord	11.97 ft	2.09 ft.
Tip chord	5.58 ft	1.045 ft.
Total flap span	67% span	67% span.
Center of gravity	25% mac	25% mac.
Hor. tail area	85.3 sq. ft	3.007 sq. ft.
C. G. to C. P. of tail	20.7 ft	3.88 ft.
l_1=prop. to C. G	11.71 ft	2.198 ft.
l_2=C. G. to elev. H. L	22.5 ft	4.205 ft.

FIGURE 3.—Three views of a 3/16-scale model of a single-engine airplane.

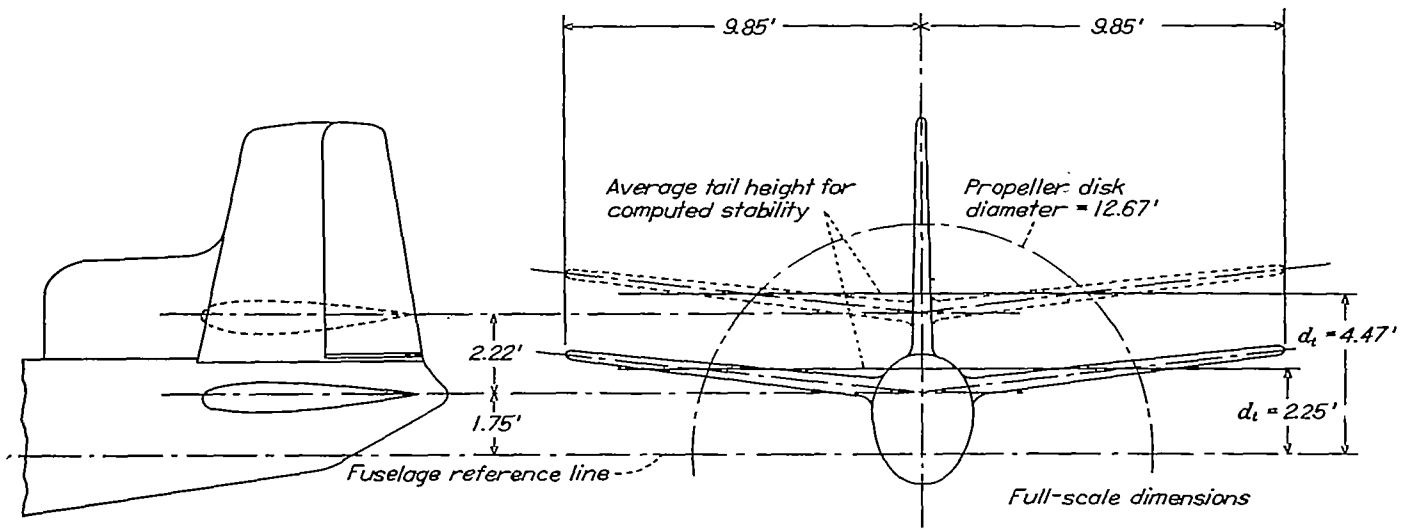

FIGURE 4.—Schematic drawing of normal and raised tail position

setting is shown on figure 7. The assumed full-scale T_c against C_L relationships for 920, 2100, and 3450 horsepower (and a wing loading of 39.2 lb./ft.^{2}) are shown in figure 8.

TESTS AND REDUCTION OF DATA

The tests consisted of a series of runs at constant values of T_c, with flaps up and flaps deflected 38°, and with the propeller tilted both −0.8° and −5.5°. These tests were made with tail removed, tail in its normal position with

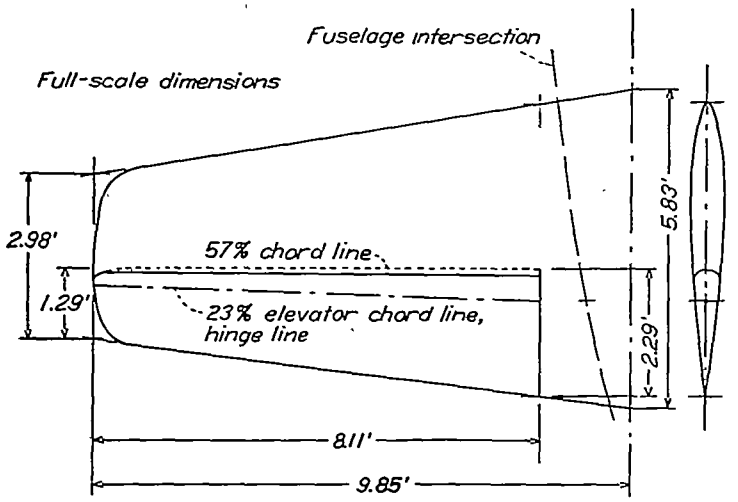

Total horizontal tail area =85.3 sq. ft.
Total elevator area aft of hinge line=23.3 sq. ft.
Average chord aft of hinge line =1.46 ft.

FIGURE 5.—Details of horizontal tail.

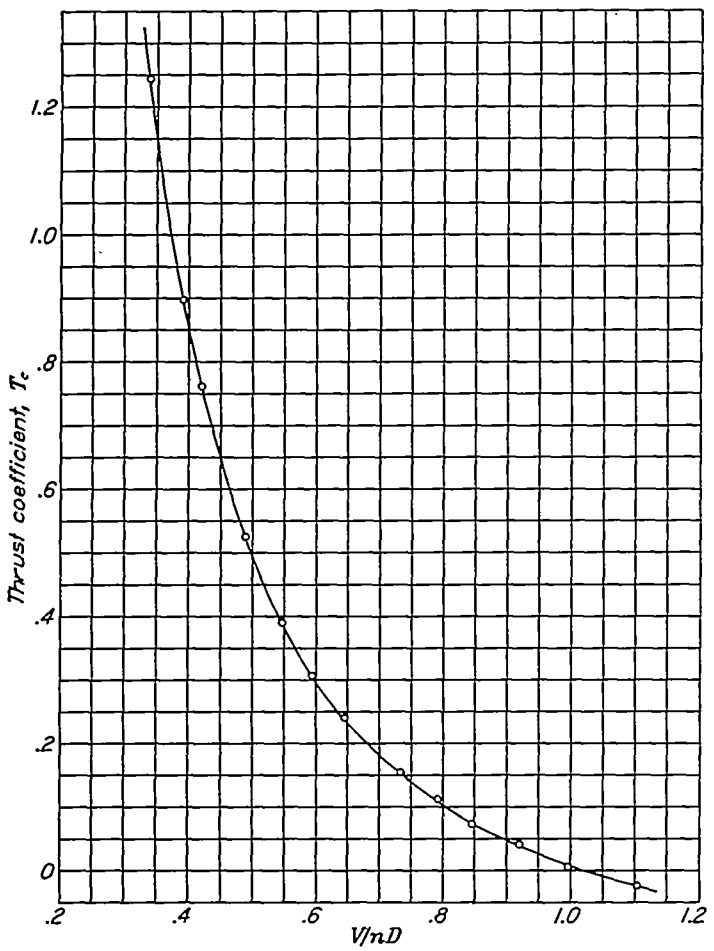

FIGURE 6.—Variation of T_c with V/nD for model propeller at a blade angle of 21° at 0.75 radius. Diameter=2.373 ft., n=100 rps.

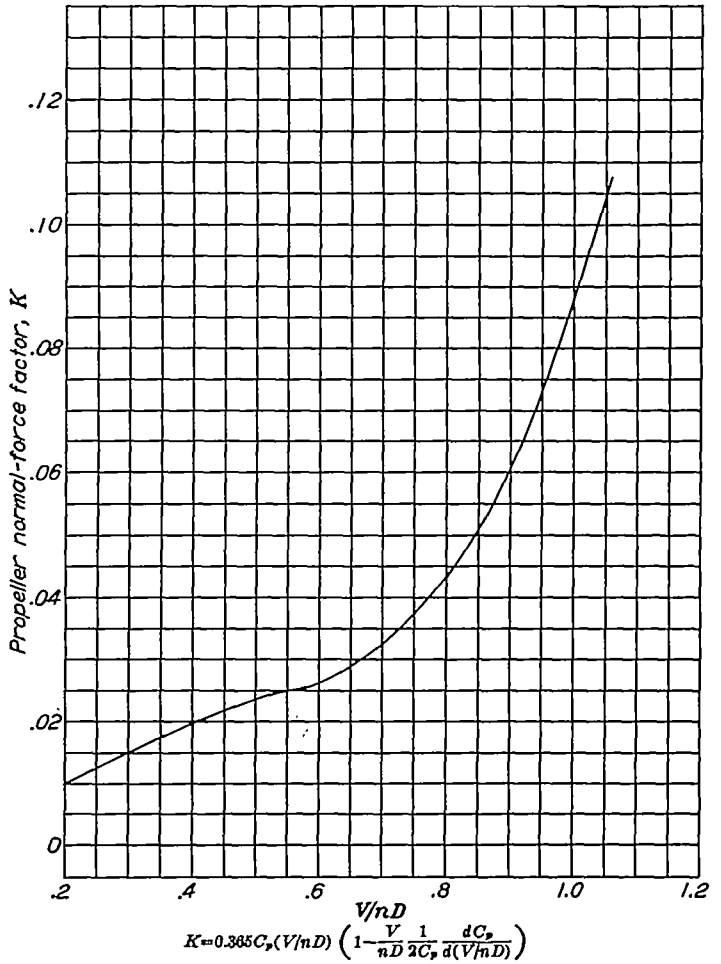

FIGURE 7.—Variation of K with V/nD for model propeller at a blade angle of 21.0° at 0.75 radius.

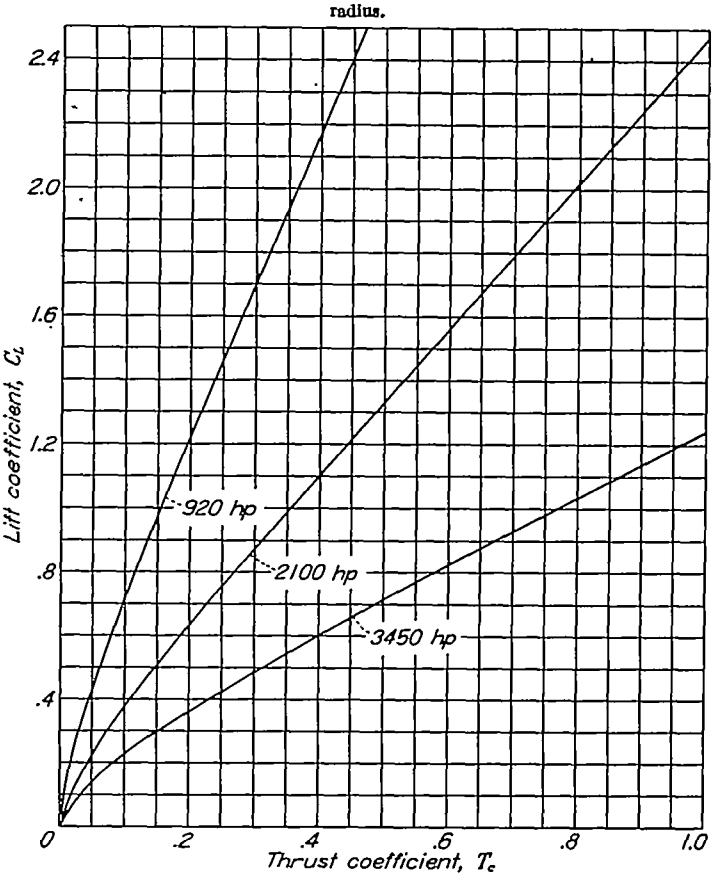

FIGURE 8.—Assumed variation of thrust coefficient with lift coefficient in steady flight for 920, 2,100, and 3,450 horsepower. Wing loading=39.2 lb./sq. ft. Propeller diameter=12.67 ft.

several elevator deflections, and tail in the raised position with neutral elevator only. A similar series of propeller-removed tests was also made.

The values of T_c were selected so that the thrust resulting from the use of 3,450 horsepower could be simulated with flaps up and 2,100 horsepower with flaps down. The various values of T_c were obtained by holding the motor power at its safe limit and adjusting the test velocity to secure the required V/nD. The test Reynolds number varied from 900,000 to 2,500,000 dependent upon the value of T_c. The results obtained in this fashion were plotted against T_c as the major variable with angle of attack as a parameter. Cross plots were then made for the preselected T_c against C_L relationships (shown in fig. 8) equivalent to 920, 2,100,

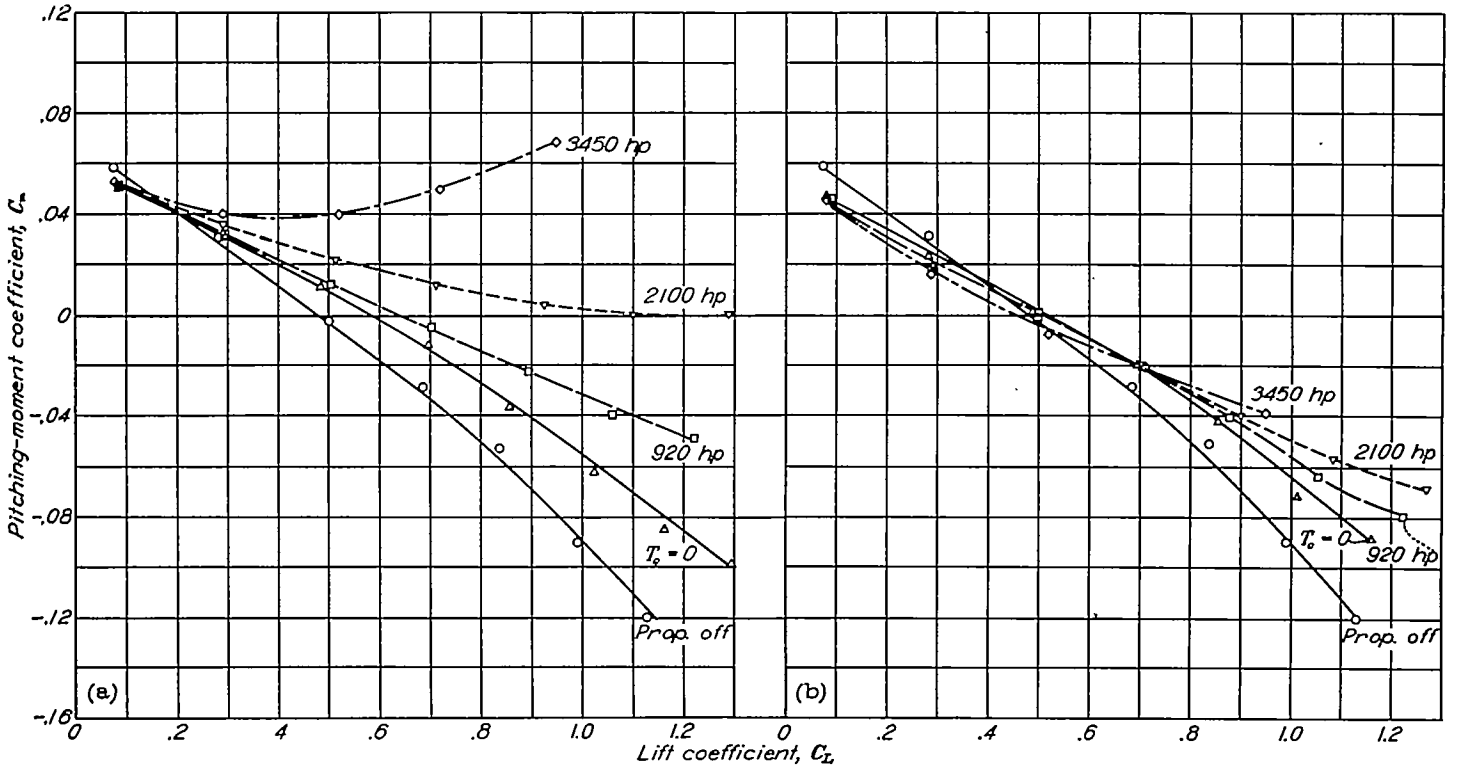

(a) Tilt of the propeller axis=−.8° (b) Tilt of the propeller axis=−5.5°

FIGURE 9.—Effect of propeller operation on longitudinal stability of a single-engine airplane with two tilts of the propeller axis. Normal tail position δ_e=0° flaps up.

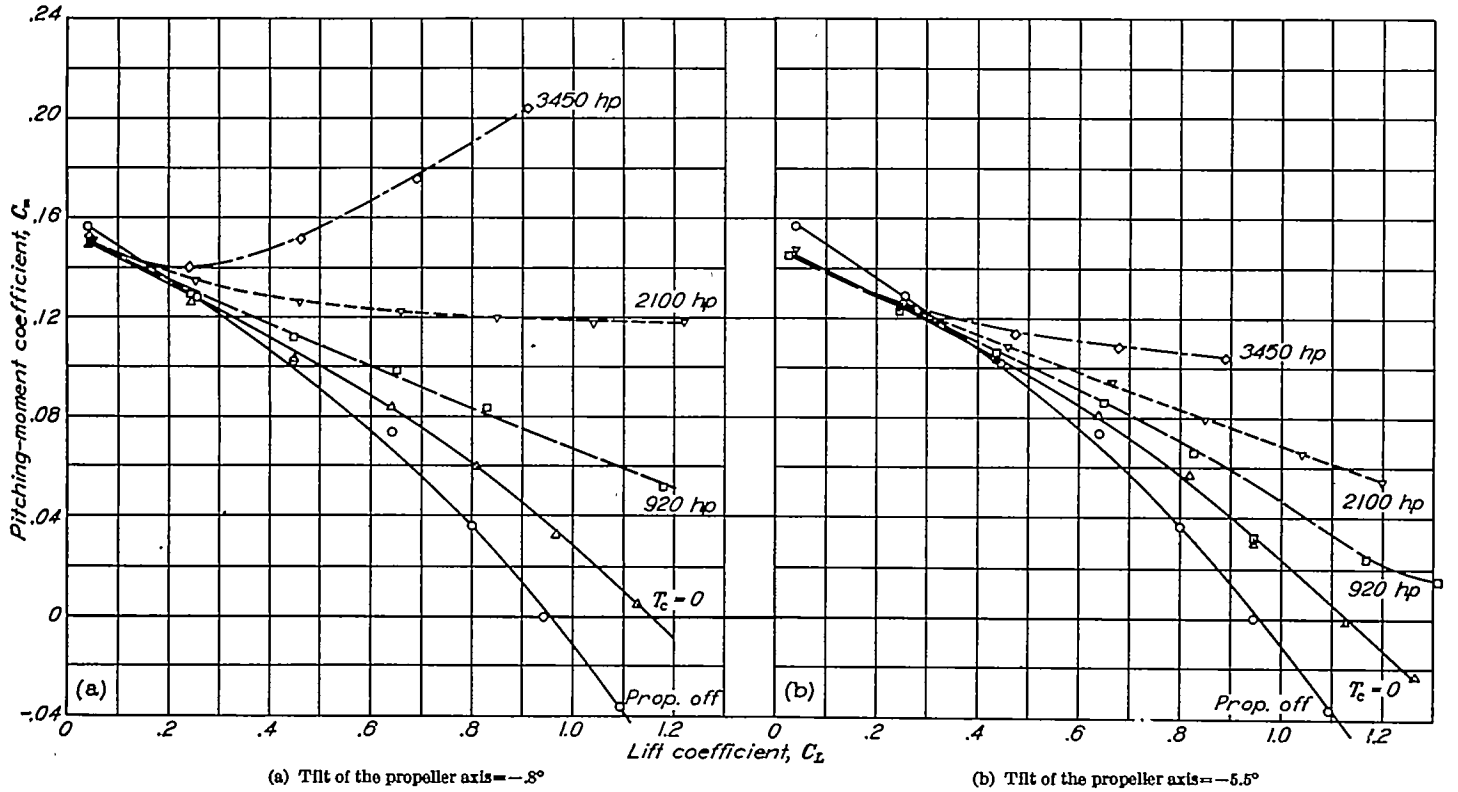

(a) Tilt of the propeller axis=−.8° (b) Tilt of the propeller axis=−5.5°

FIGURE 10.—Effect of propeller operation on longitudinal stability of a single-engine airplane with two tilts of the propeller axis. Normal tail position δ_e=−5° flaps up.

and 3,450 horsepower. The results of these cross plots, which are equivalent to the conventional constant-power polars, are presented herein.

RESULTS AND DISCUSSION

PITCHING MOMENT, FLAPS UP

The effect of propeller operation on the pitching moment of the model (tail in normal position) with two different propeller tilts is shown in figures 9 to 11. The shift in neutral point at various lift coefficients, as determined from dC_m/dC_L about the 0.25 M. A. C. point with elevator deflected for trim, is shown on figure 12.

From inspection of these figures the beneficial effect of tilt of the propeller axis is evident. The characteristic destabilizing effect of power is present with the −0.8° tilt, while with the −5.5° tilt it is either considerably decreased or

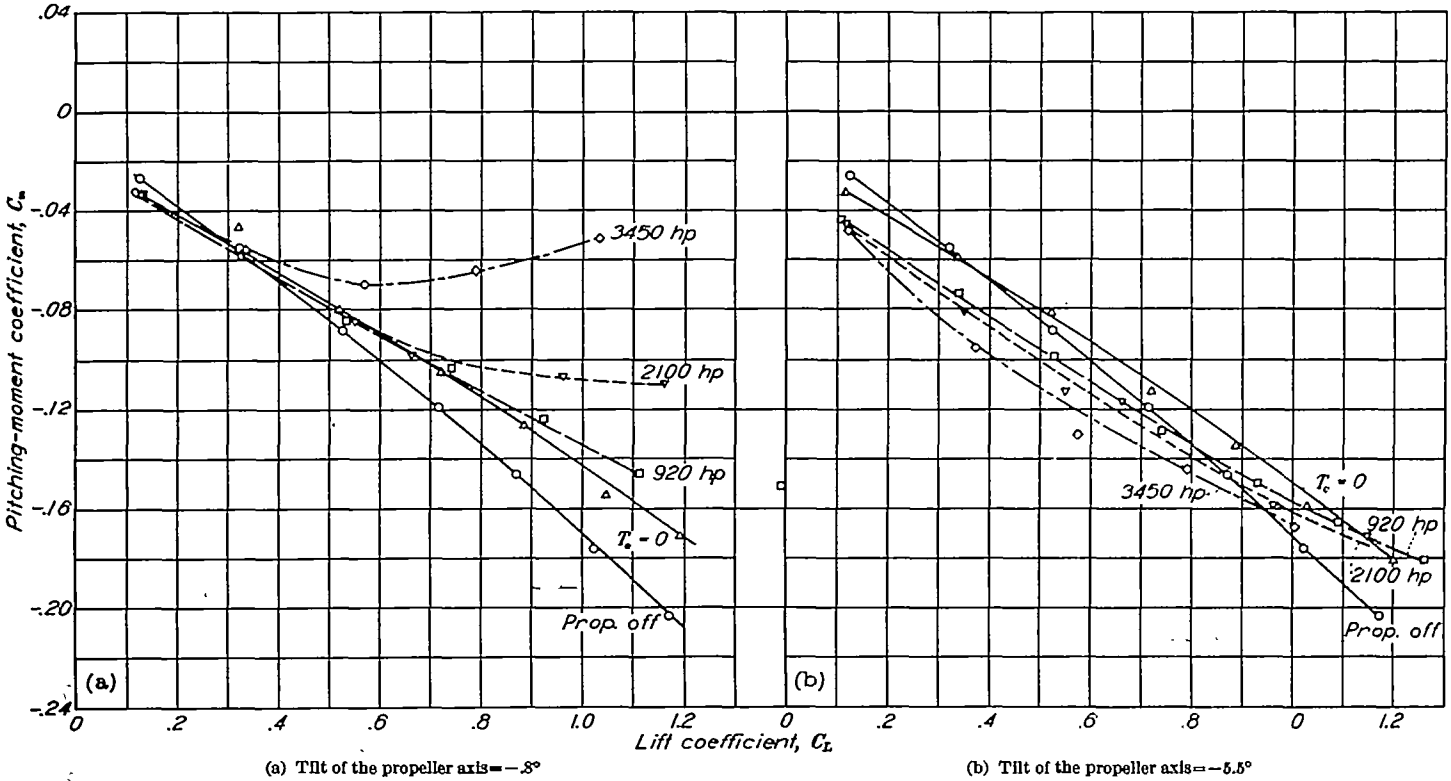

(a) Tilt of the propeller axis=−.8° (b) Tilt of the propeller axis=−5.5°

FIGURE 11.—Effect of propeller operation on longitudinal stability of a single-engine airplane with two tilts of the propeller axis. Normal tail position δ_t=5° flaps up.

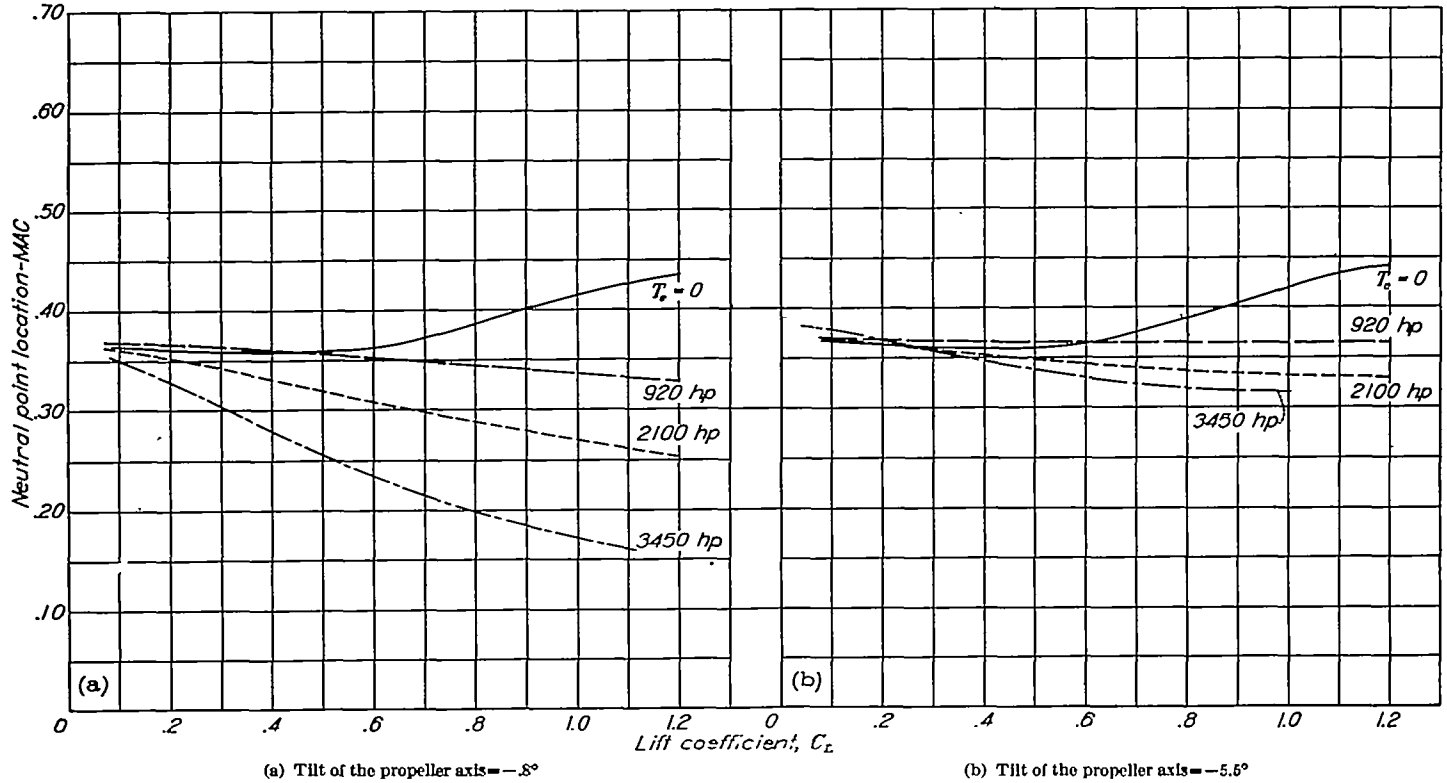

(a) Tilt of the propeller axis=−.8° (b) Tilt of the propeller axis=−5.5°

FIGURE 12.—Effect of propeller operation on neutral point location of a single-engine airplane with two tilts of the propeller axis. Normal tail position—elevator deflected to trim—flaps up.

entirely eliminated, dependent on the load carried by the tail (as determined by the elevator deflection). It will be observed from figure 12 (a) that, at a C_L of 0.8, the application of 2,100 horsepower causes a forward shift in neutral point of 0.10 M. A. C. with the −0.8° tilt in contrast to 0.05 M. A. C. shift with the −5.5° tilt. Thus, the beneficial effect of the tilt is equivalent to a shift in the neutral point of 0.05 M. A. C. compared to the possible 0.06 M. A. C. shift discussed in the Introduction. A more extended comparison of experimental and computed results is given in the section Application to Other Designs. As indicated therein the correspondence between the computed and experimental results varies somewhat, dependent on the power and C_L. However, in general, the correspondence tends to be best at the higher powers where the effects are greatest.

From the data presented in figure 13 (for tail off) and

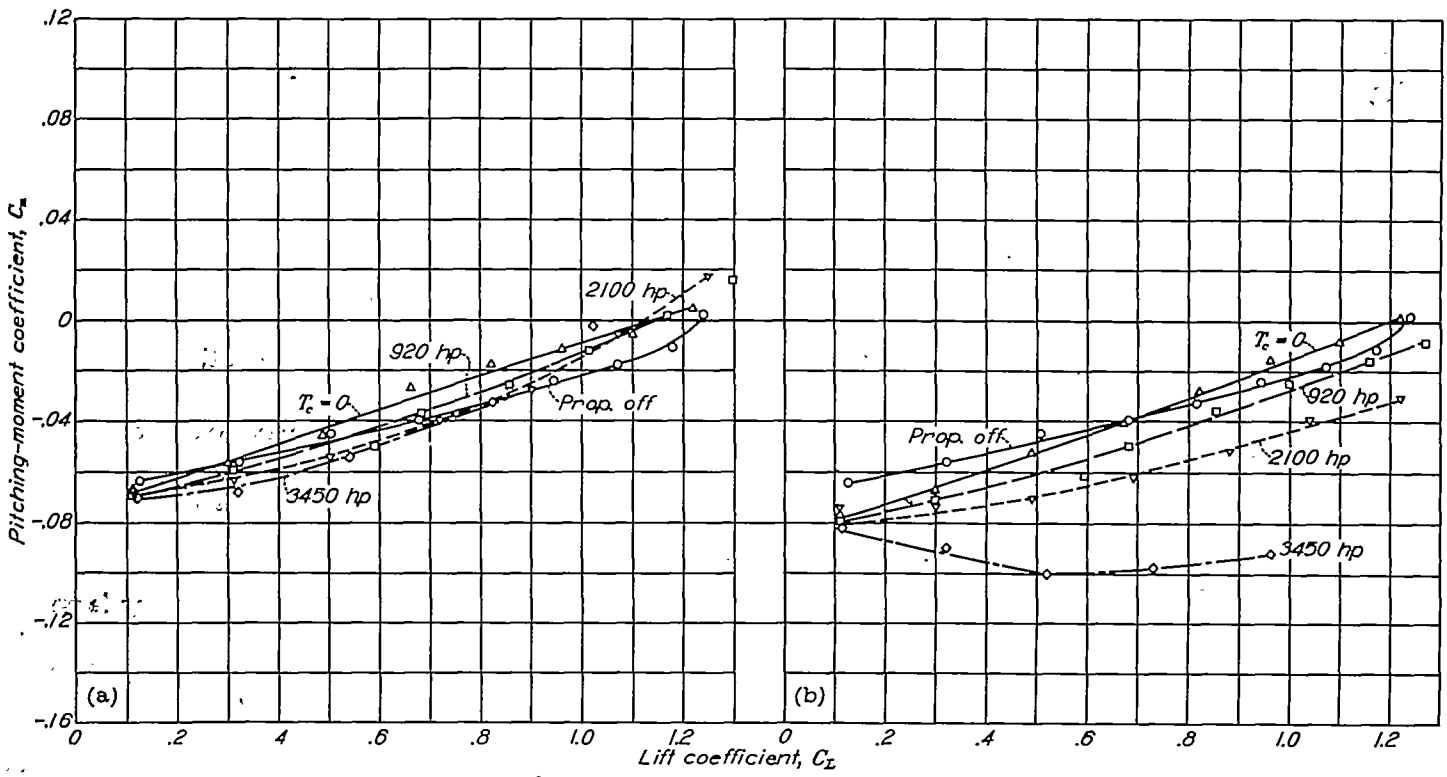

(a) Tilt of the propeller axis=−.8°

(b) Tilt of the propeller axis=−5.5°

FIGURE 13.—Effect of propeller operation on longitudinal stability of a single-engine airplane with two tilts of the propeller axis. Tail off, flaps up.

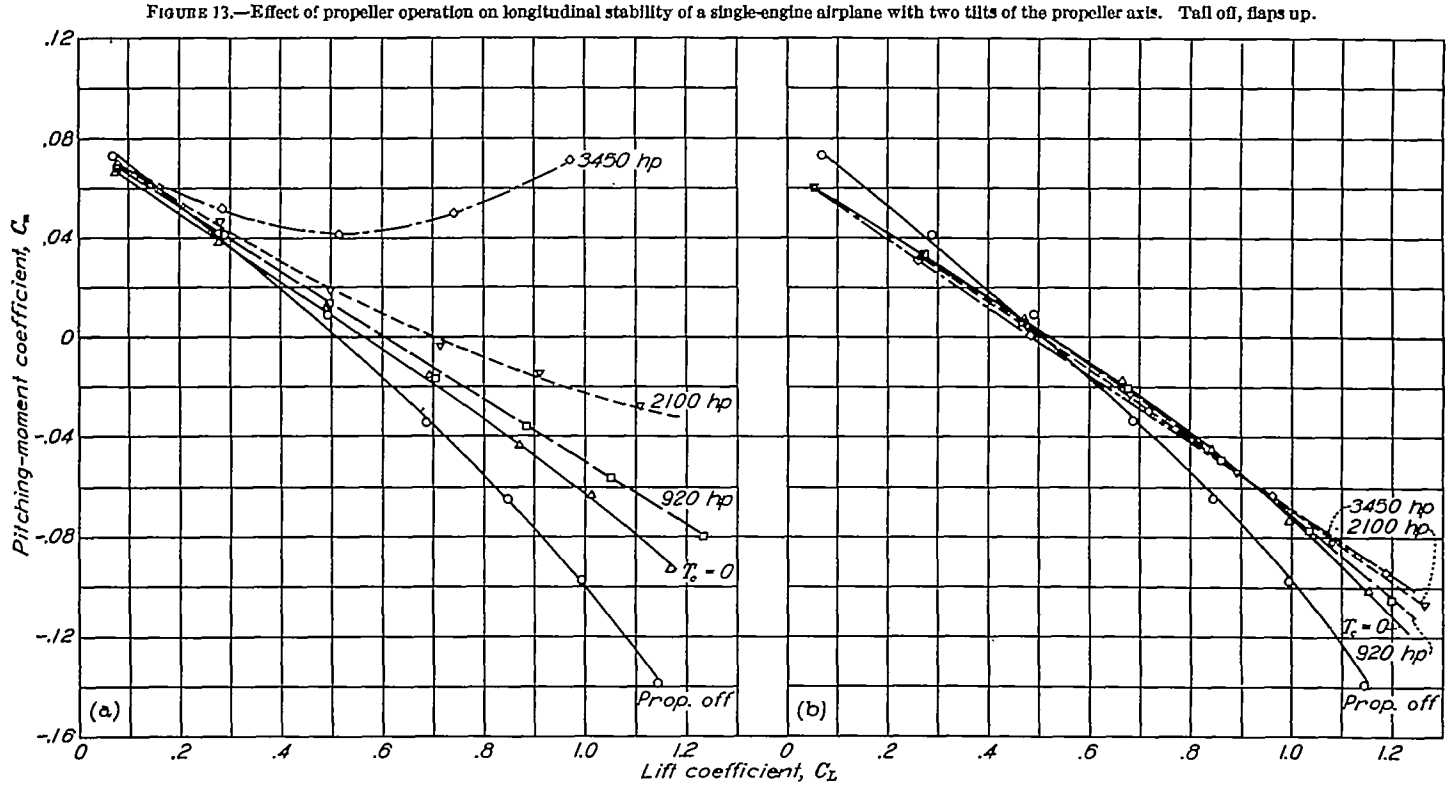

(a) Tilt of the propeller axis=−.8°

(b) Tilt of the propeller axis=−5.5°

FIGURE 14.—Effect of propeller operation on longitudinal stability of a single-engine airplane with two tilts of the propeller axis. Raised tail position, i_t=0°, flaps up.

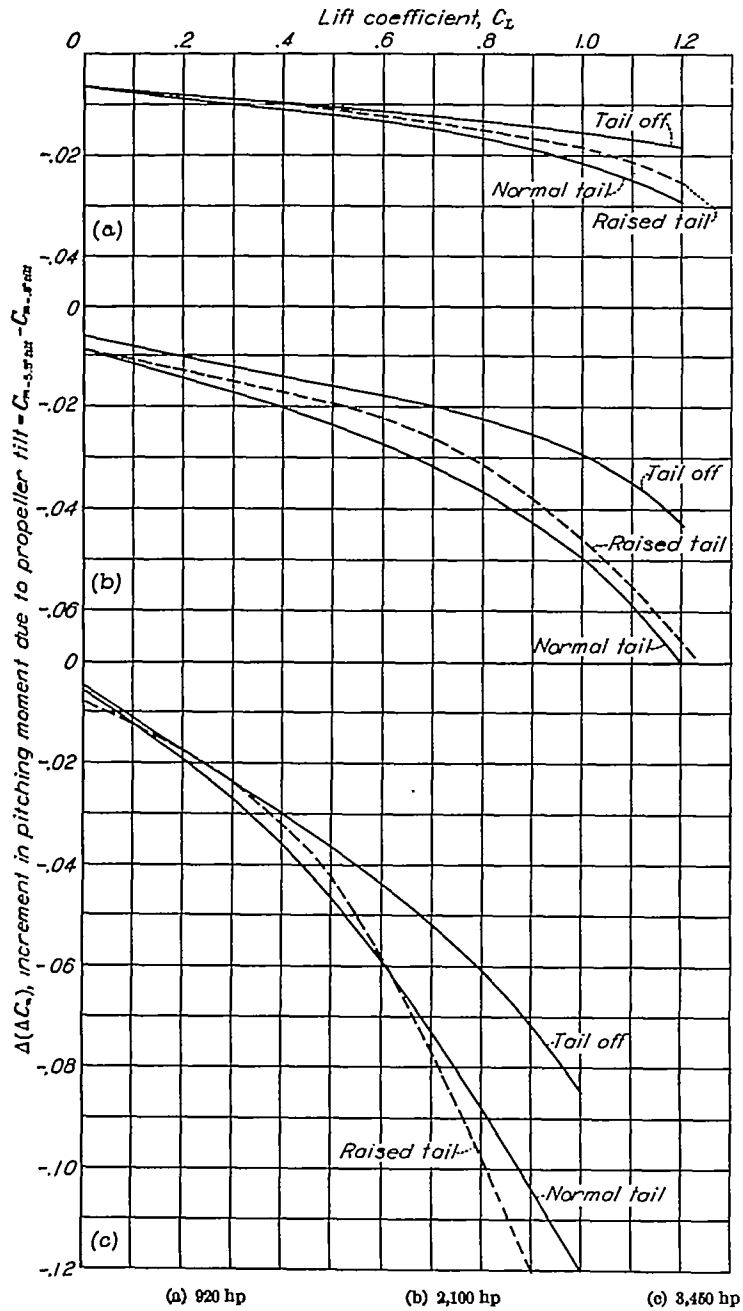

FIGURE 15.—Experimental increment in pitching moment due to propeller tilt. Flaps up, tail off, and tail on with elevator neutral.

figure 14 (tail in the raised position), it is possible to determine the extent to which these affects are due to the direct propeller forces and the influence of the tail height on the tail effects. The incremental effects of the tilt of the propeller have been determined from the data of figures 9, 13, and 14, and are presented in figure 15 in the form of $\Delta(\Delta C_m)$ against C_L. It will be observed that the direct effects of the propeller tend to predominate over the tail effects. The increase in tail height causes a decrease in the beneficial effect of the tilt, mainly, because with the higher tail position the over-all destabilizing effects of power are somewhat less; therefore, there is less to be gained by a change. A more detailed analysis of this is given in the section Application to Other Designs along with a comparison of the experimental and computed results. It is shown there that the normal tail is in such a position as to suffer the greatest effects of power; therefore, the effect of the tilt on the tail pitching moment shown on figure 15 is probably the maximum which will be measured for any tail height.

PITCHING MOMENT, FLAPS DEFLECTED 38°

The effect of propeller operation on the pitching moment of the model with flaps deflected is shown in figures 16 to 20. The location of the neutral point at various lift coefficients as determined from dC_m/dC_L with elevator deflected for trim is shown on figure 21.

The trend of the results is the same as that observed with flaps up. In a typical approach condition (920 hp. at a C_L of 2.0) a favorable neutral point shift due to the tilt of as much as 0.035 M. A. C. is realized. With 2100 horsepower the shift is 0.05 M. A. C. at this C_L. Figure 22 shows that the major portion of the increase in stability came from the direct propeller forces. The $\Delta(\Delta C_m)$ with tail off is very nearly equal to that with tail on up to a C_L of 1.6. As will be shown later this is due to the fact that the slipstream passes under the tail, and thus there is very little difference in the change in pitching moment resulting from the tilt for the two tail heights.

EFFECT ON HINGE MOMENT AND LIFT

Elevator hinge moment for flaps up and flaps deflected 38° is presented in figures 23 and 24. There is little or no change due to tilting the thrust line. This might be expected since dC_{h_e}/di_t is small for the model tested and the average velocity over the tail is not changed to a very large extent due to tilt.

The maximum lift coefficient, tail off, was decreased 0.06 for flaps retracted and 0.07 for flaps deflected with 2,100 horsepower (fig. 25). The decrease in lift is directly traceable to the change in the vertical component of the thrust and normal force. The low-power maximum lift, which will be more frequently used, is decreased about 0.04, probably a negligible amount.

EFFECT ON THE LONGITUDINAL HANDLING QUALITIES

The longitudinal handling qualities were predicted for flaps up (fig. 26) and flaps deflected (fig. 27) from the data previously presented for the various power conditions tested.

Flaps retracted.—The stick force against velocity curves were computed for trim at C_L=0.6 which corresponds to a velocity of 160 miles per hour, a normal climb speed. Figure 26 (a) shows that, with −0.8° tilt, there is marginal stick-free stability with 2,100 horsepower, while with 3,450 horsepower marked instability exists. In contrast to this, with −5.5° tilt (fig. 26 (b)), considerable stability exists for the 2,100-horsepower conditions and the airplane becomes only marginally stable with 3,450 horsepower. It is obvious from the previous discussion that, since the tilt of the propeller axis does not affect the elevator hinge moments, all the change in the stick-free characteristics is due to the increase in the slope of C_m against C_L. The increased variation of δ_e with V_i resulting therefrom (fig. 26) causes the more stable variation of stick force with V_i.

As was pointed out in the Introduction, the maintenance of stability in the high-power low-speed condition necessitates that a high degree of stability be present under conditions where the power effects are small (e. g., high speed). This condition is evident in figure 26 (a) where, in order to obtain

just marginal stability with 2,100 horsepower, the basic stability must be so high that an excessive stick force per g (30 lb.) is present in high-speed maneuvers. If advantage is taken of the decreased effect of power made possible by the tilted propeller, the basic stability can be considerably decreased with a consequent reduction of the stick force per g. The decrease in stability normally would be secured by a decreased tail size, so that not only would a reduction in stick force result from a decreased dC_m/dC_L but also from the decreased area of the elevator. The precise evaluation of such a saving could only be made by testing a reduced size tail. However, a result (which will be on the conservative side) can be obtained from the data available if the decrease in dC_m/dC_L is assumed to come from a rearward movement of the center of gravity. (The advantage gained from reduced elevator area is not included in this procedure.) The char-

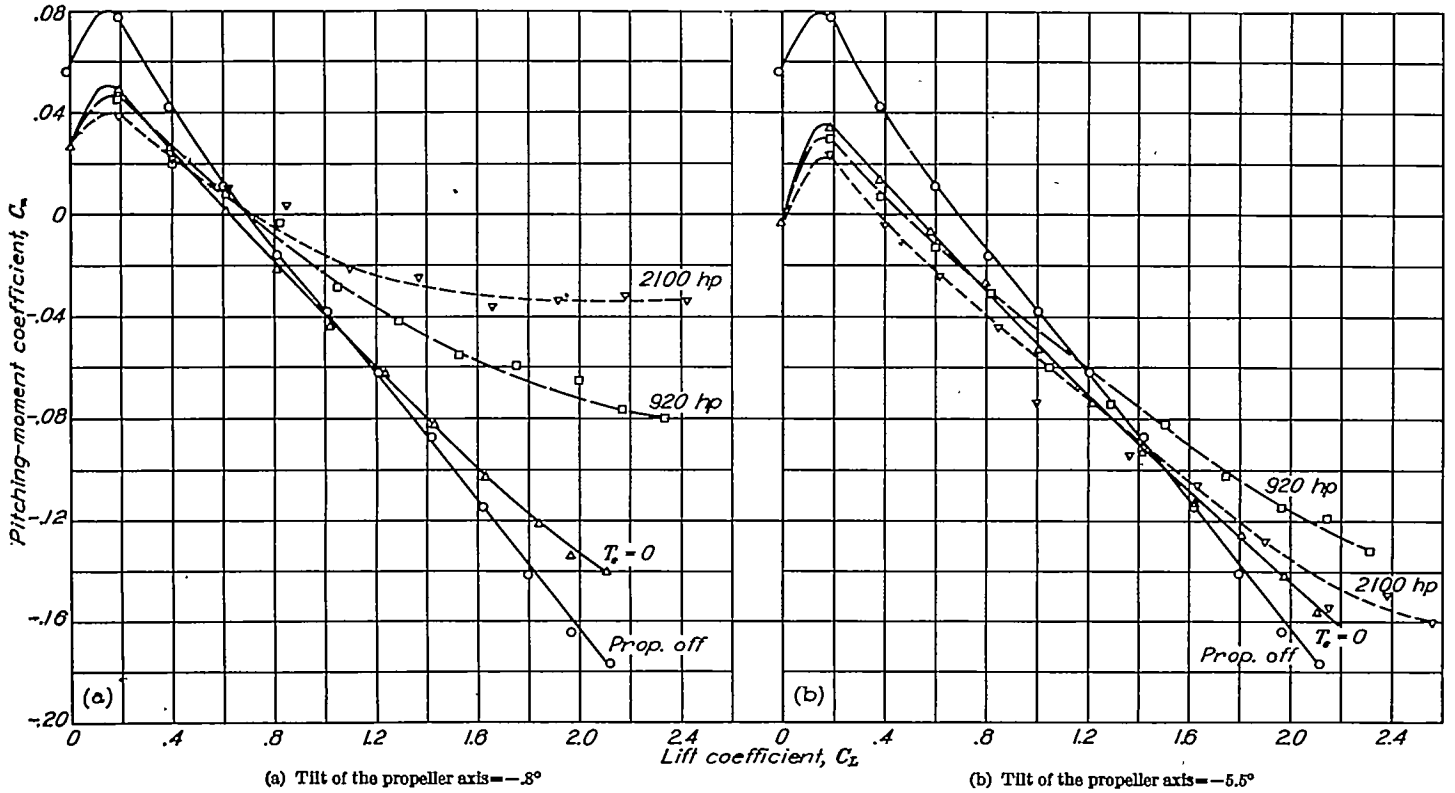

(a) Tilt of the propeller axis=—.8° (b) Tilt of the propeller axis=—5.5°

FIGURE 16.—Effect of propeller operation on longitudinal stability of a single-engine airplane with two tilts of the propeller axis. Normal tail position δ_e=0° flaps deflected 38°.

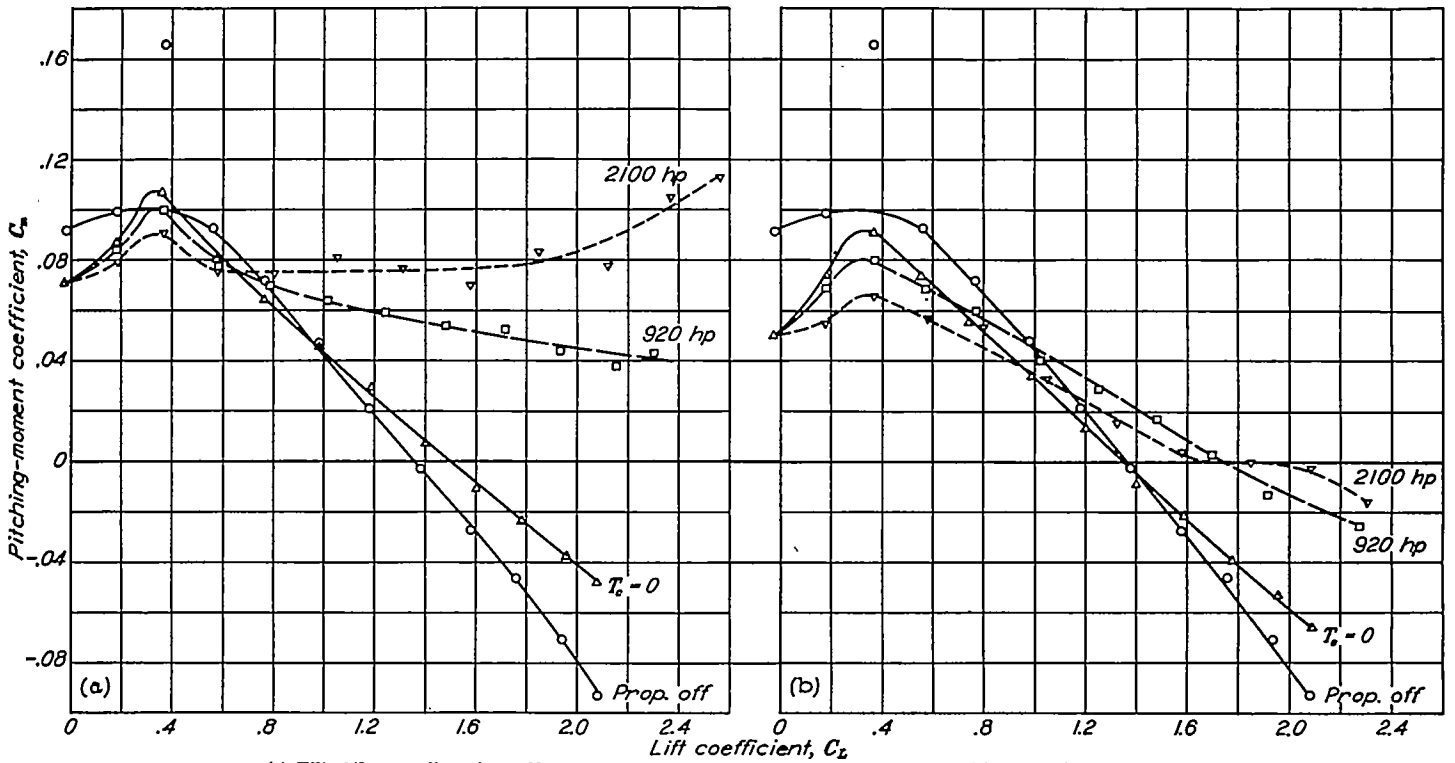

(a) Tilt of the propeller axis=—.8° (b) Tilt of the propeller axis=—5.5°

FIGURE 17.—Effect of propeller operation on longitudinal stability of a single-engine airplane with two tilts of the propeller axis. Normal tail position δ_e=—5° flaps deflected 38°.

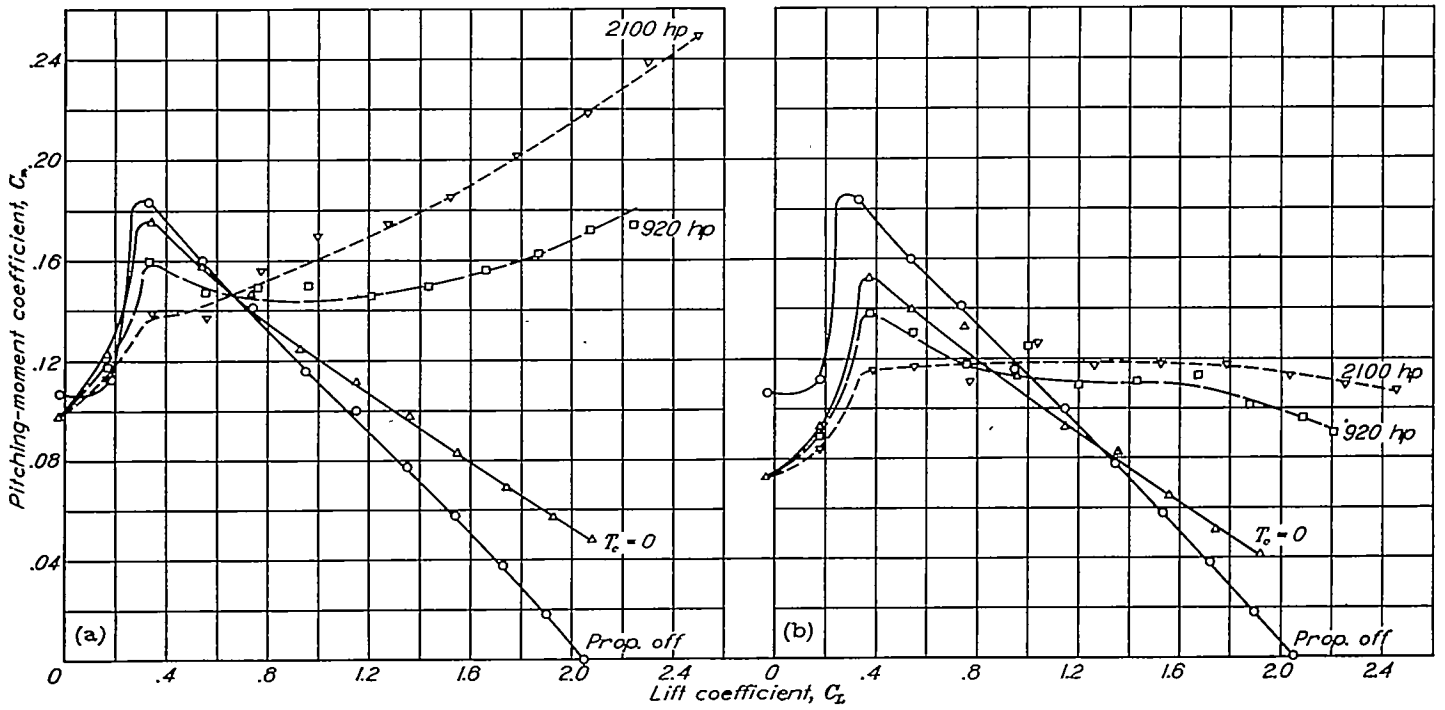

(a) Tilt of the propeller axis=−.8°

(b) Tilt of the propeller axis=−5.5°

FIGURE 18.—Effect of propeller operation on longitudinal stability of a single-engine airplane with two tilts of the propeller axis. Normal tail position δ_t=−10° flaps deflected 38°.

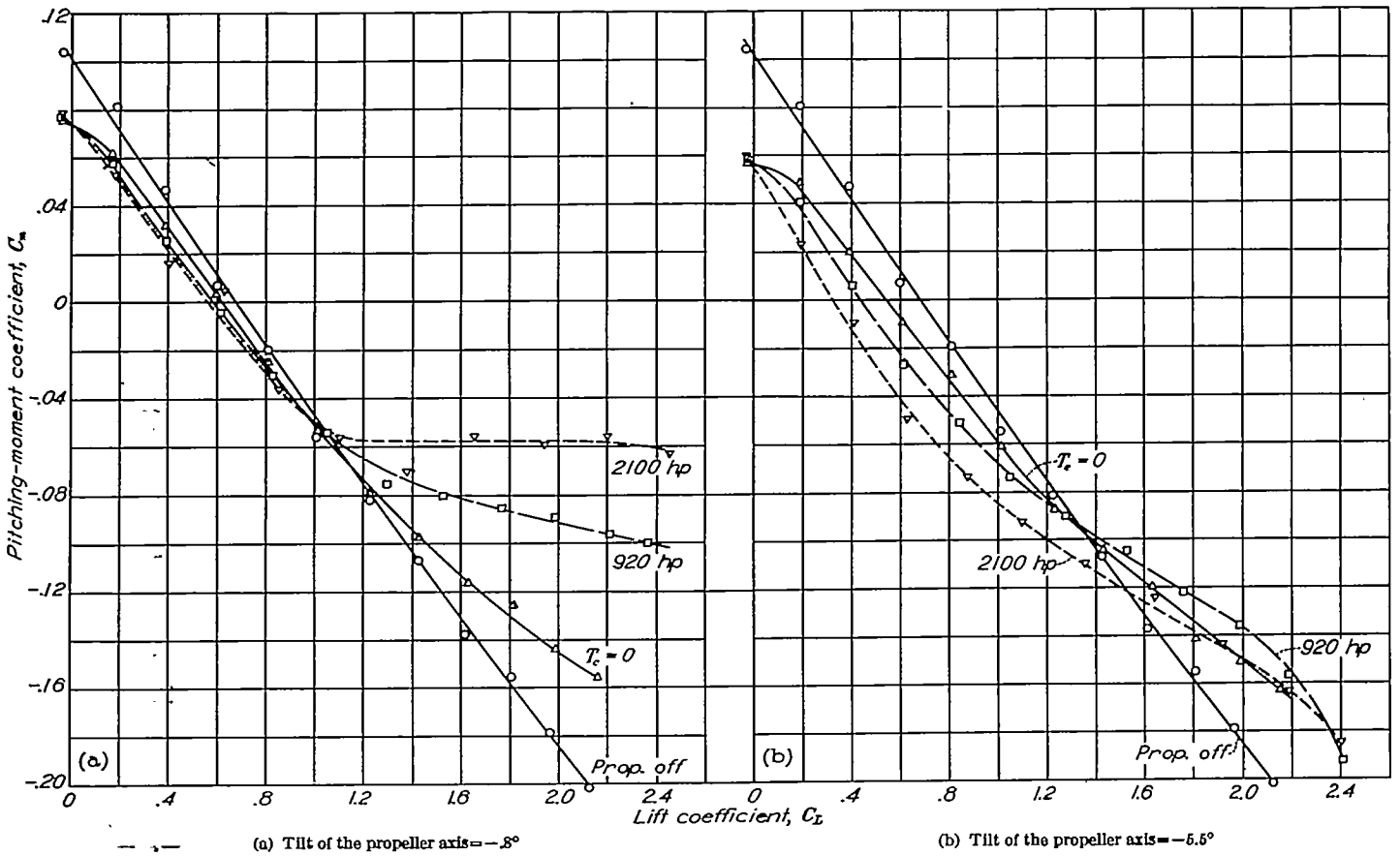

(a) Tilt of the propeller axis=−.8°

(b) Tilt of the propeller axis=−5.5°

FIGURE 19.—Effect of propeller operation on longitudinal stability of a single-engine airplane with two tilts of the propeller axis. Raised tail position δ_t=0° flaps deflected 38°.

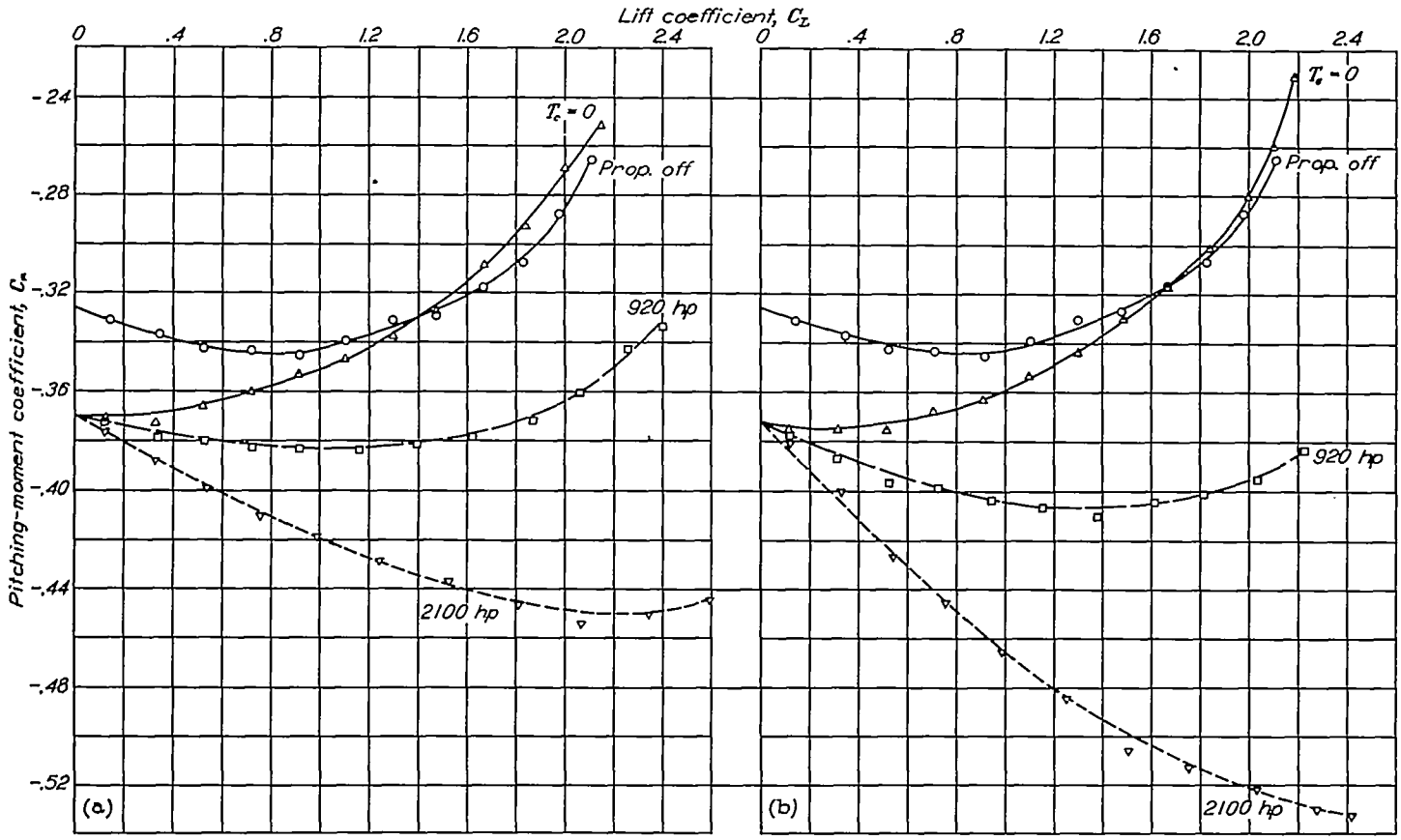

(a) Tilt of the propeller axis=−.8°

(b) Tilt of the propeller axis=−5.5°

FIGURE 20.—Effect of propeller operation on longitudinal stability of a single-engine airplane with two tilts of the propeller axis. Tail off, flaps deflected 38°.

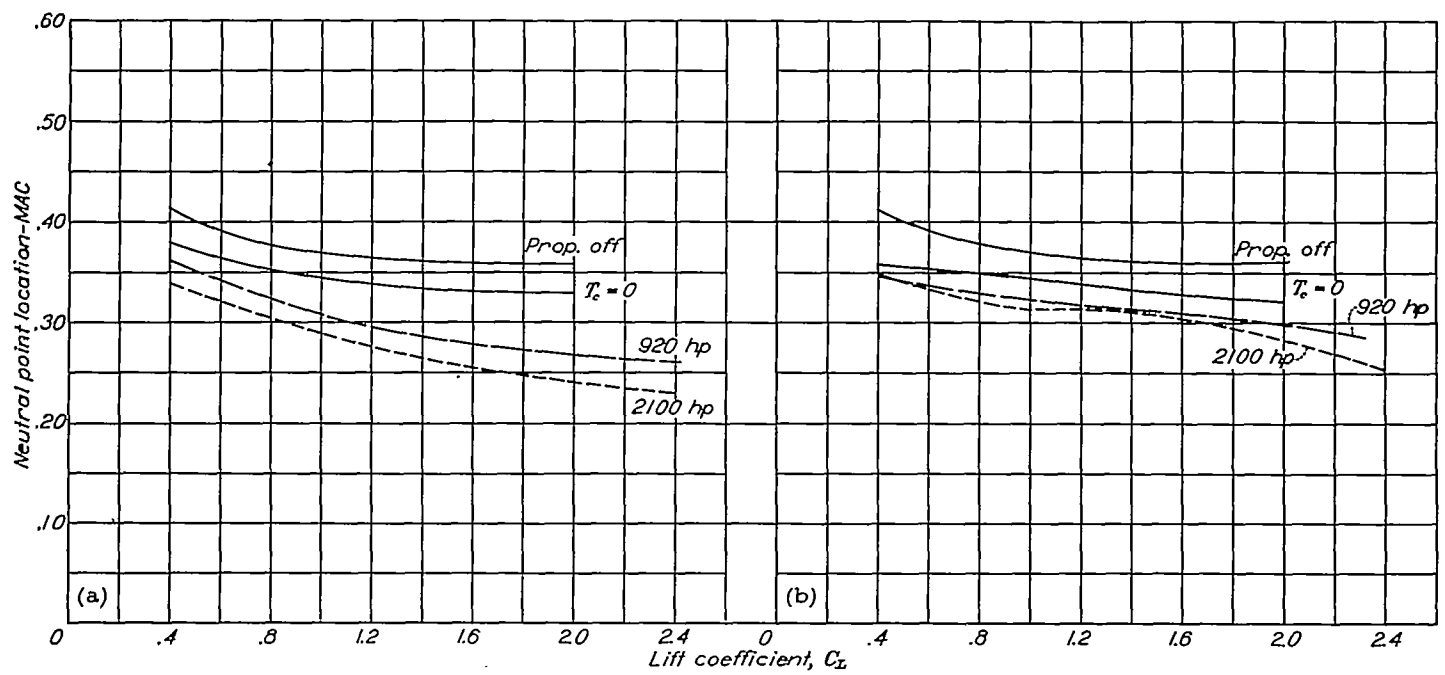

(a) Tilt of the propeller axis=−.8°

(b) Tilt of the propeller axis=−5.5°

FIGURE 21.—Effect of propeller operation on neutral point location of a single-engine airplane with two tilts of the propeller axis. Normal tail position, elevator deflection to trim, flaps deflected 38°.

acteristics for a 0.30 M. A. C. center-of-gravity position with −5.5° tilt of the propeller are shown on figure 26 (c). It will be noted that the stick force against velocity characteristics remain more stable than for the −0.8 tilt and 0.25 M. A. C. center-of-gravity position; and, in addition, a reduction of 10 pounds per g is realized in the stick force in maneuvers.

Flaps deflected.—The stick force against velocity was computed for a typical approach condition with the elevator assumed trimmed for a C_L=1.0 and a velocity of 124 miles per hour. In this attitude if there is a balked landing requiring the application of power or if power must be applied to maintain a given sinking speed, the airplane will become marginally stable with 920 horsepower at 120 miles per hour and will be unstable throughout the speed range with 2,100 horsepower (fig. 27(a)). In contrast, tilting the propeller gives satisfactory stability for 920 horsepower and marginal stability at about 90 miles per hour with 2,100 horsepower (fig. 27(b)).

APPLICATION TO OTHER DESIGNS

It is the purpose of this section to show the comparison between experimental results and those which would be predicted from available theory. The demonstration of the computation of the results from this theory serves to illustrate the methods by which the effect of tilting the propeller can be estimated for other designs.

The computation methods follow in general those outlined in reference 1, with some modification in detail. These computations naturally divide themselves into two parts: one dealing with the effects due to the direct propeller forces, the other dealing with the effects resulting from the changes in the slipstream insofar as it influences the contribution of pitching moment by the tail.

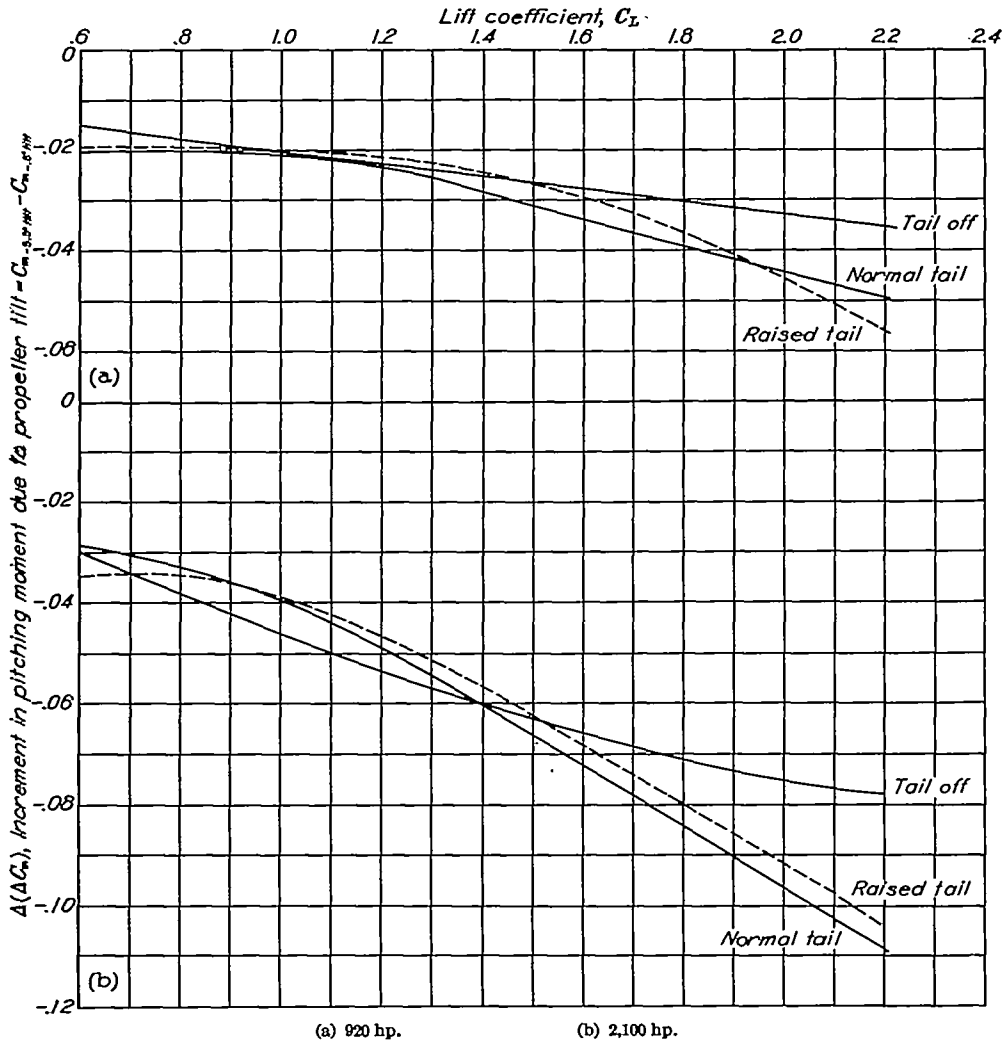

(a) 920 hp. (b) 2,100 hp.

FIGURE 22.—Experimental increment in pitching moment due to propeller tilt. Flaps 38°, tail off and tail on with elevator undeflected.

EFFECTS OF DIRECT PROPELLER FORCES

Following conventional practice, the propeller forces can be broken down into the component acting along the thrust axis and the component normal to the thrust axis. From reference to figure 1, it is evident that the moment about the center of gravity produced by these forces will be as follows:

$$\Delta M_{prop}=Tz+N_P l_1 \tag{1}$$

$$\Delta C_{m_{prop}}=\frac{Tz}{\frac{1}{2}\rho V^2 Sc}+\frac{N_P l_1}{\frac{1}{2}\rho V^2 Sc} \tag{2}$$

Substituting for T and N the relations

$$T=T_c\,\rho V^2 D^2 \tag{3}$$

$$N_P=C_{N_P}\,\rho n^2 D^4=K\sin\theta\,\rho n^2 D^4 \text{ (See note.)} \tag{4}$$

NOTE.—The expression for the normal-force component is derived by the method of Glauert as described in reference 2 (pp. 351–357) and as applied in reference 1. An alternate method which could be used with equally satisfactory results is the more recent development of Ribner (references 3, 4, and 5). Several trials have shown that the results obtained by either of the methods deviate about equal amounts from experimental results, provided the K used in Glauert's method is derived from a Cp against V/nD curve of the actual propeller used. If such data are not available, the modification of the K of a known propeller by Ribner's "side-force factor" (reference 5) to take care of blade-shape differences gives satisfactory results.

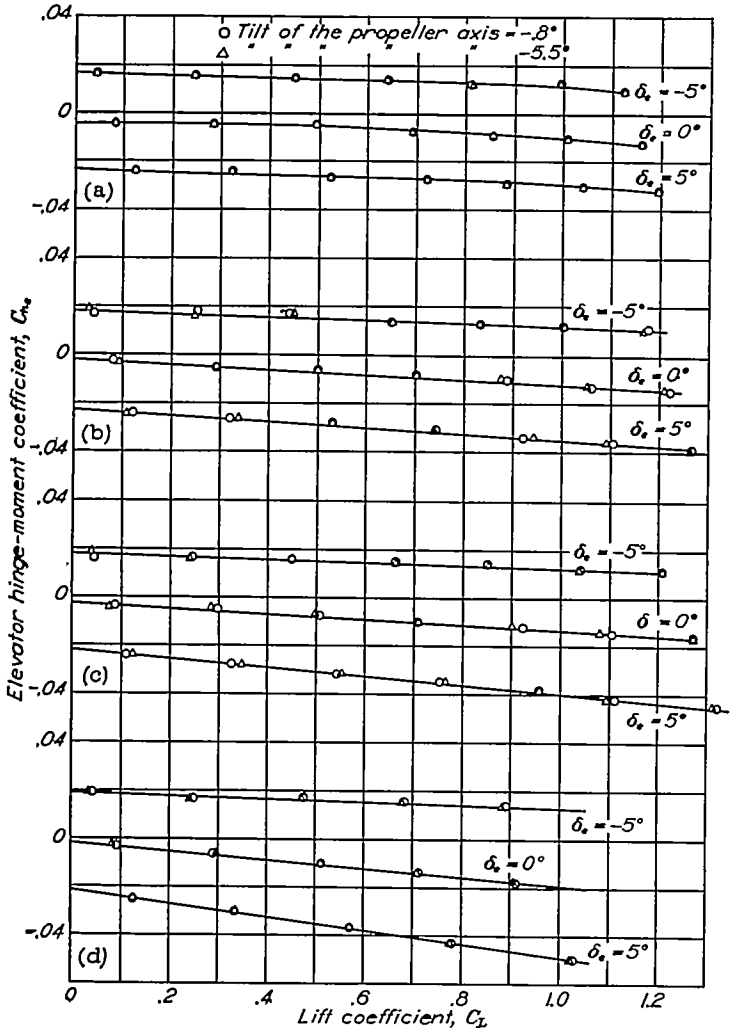

(a) T_c=0 (b) 920 hp. (c) 2,100 hp. (d) 3,450 hp.

FIGURE 23.—Effect of propeller operation on elevator hinge moment of a single-engine airplane with two tilts of the propeller axis. Normal tail position, flaps up.

gives the following:

$$\Delta C_{m_{prop}}=\underbrace{T_c\frac{2D^2}{S}\frac{z}{c}}_{\substack{\text{Effect due}\\ \text{to thrust}}}+\underbrace{\frac{K\sin\theta}{(V/nD)^2}\frac{2D^2}{S}\frac{l_1}{c}}_{\substack{\text{Effect due to}\\ \text{normal force}}} \tag{5}$$

For the purpose of determining the effect of propeller tilt, the absolute magnitude of $\Delta C_{m_{prop}}$ is not of interest. Rather, the difference in $\Delta C_{m_{prop}}$, due to the tilt of the

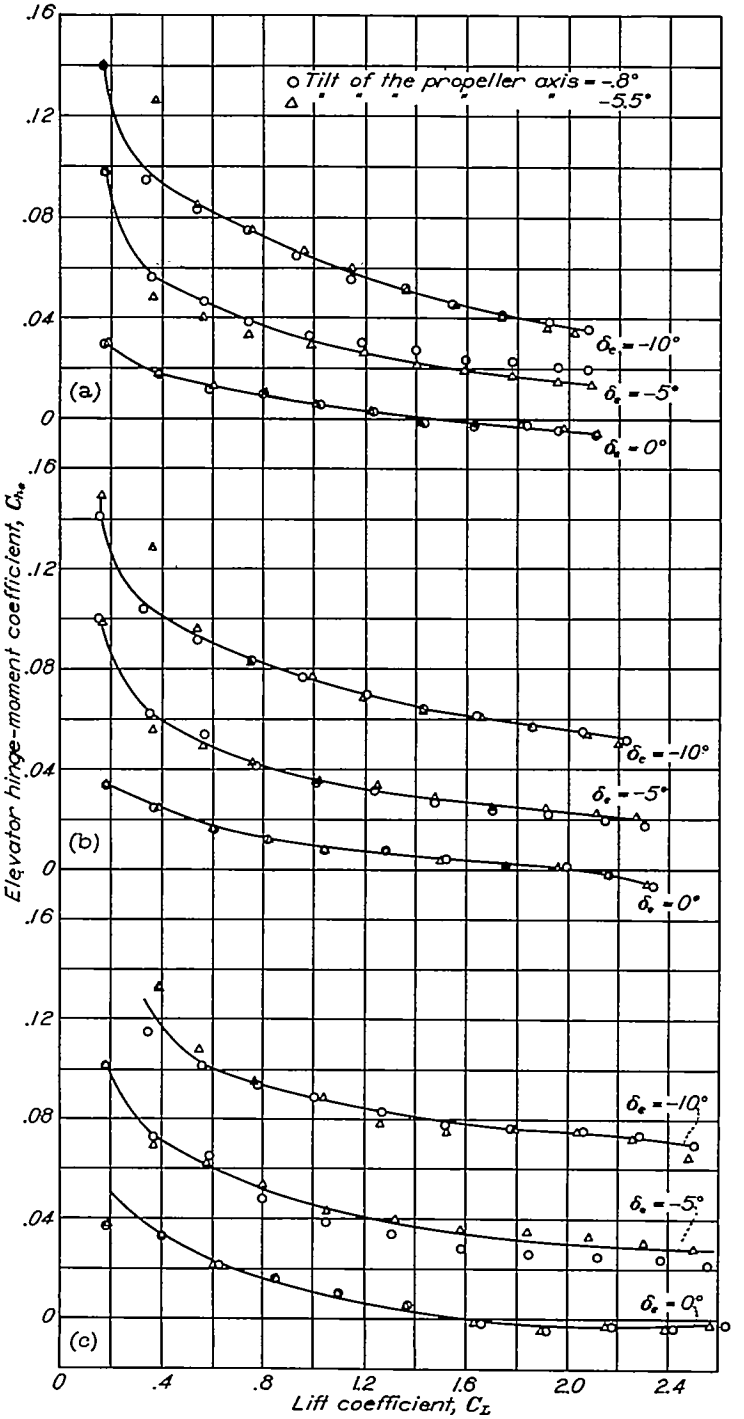

(a) T_c=0 (b) 920 hp. (c) 2,100 hp.

FIGURE 24.—Effect of propeller operation on elevator hinge moment of a single-engine airplane with two tilts of the propeller axis. Normal tail position, flaps deflected 38°.

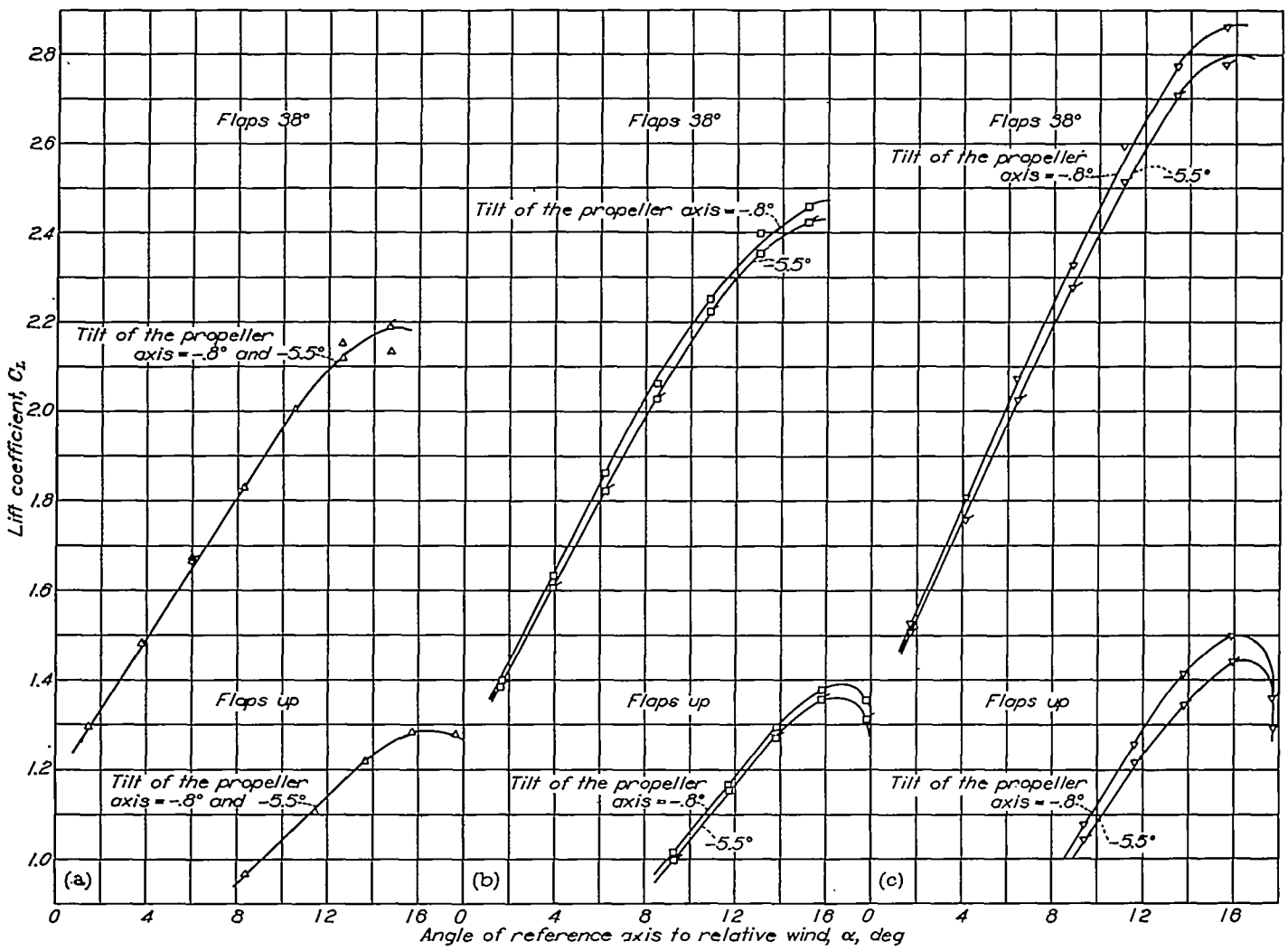

(a) T_c=0 (b) 920 hp. (c) 2,100 hp.

FIGURE 25.—Effect of tilt of propeller axis on the maximum lift coefficient of a single-engine airplane for three power conditions. Tail off, flaps up and flaps deflected 38°.

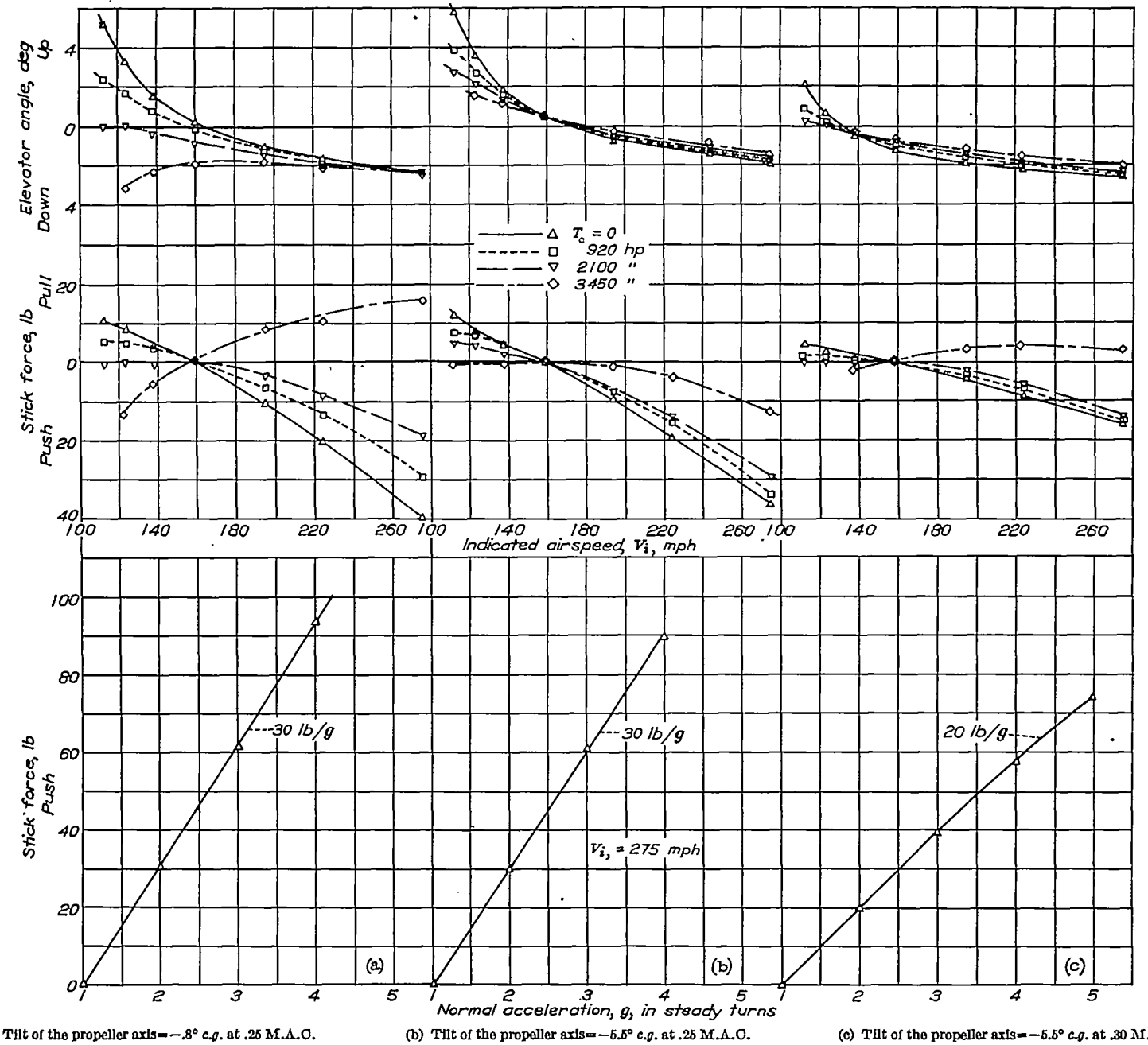

(a) Tilt of the propeller axis = −.8° *c.g.* at .25 M.A.C. (b) Tilt of the propeller axis = −5.5° *c.g.* at .25 M.A.C. (c) Tilt of the propeller axis = −5.5° *c.g.* at .30 M.A.C

FIGURE 26.—Effect of propeller operation on longitudinal handling characteristics of a single-engine airplane with two tilts of the propeller axis. Steady flight normal tail position, flaps up.

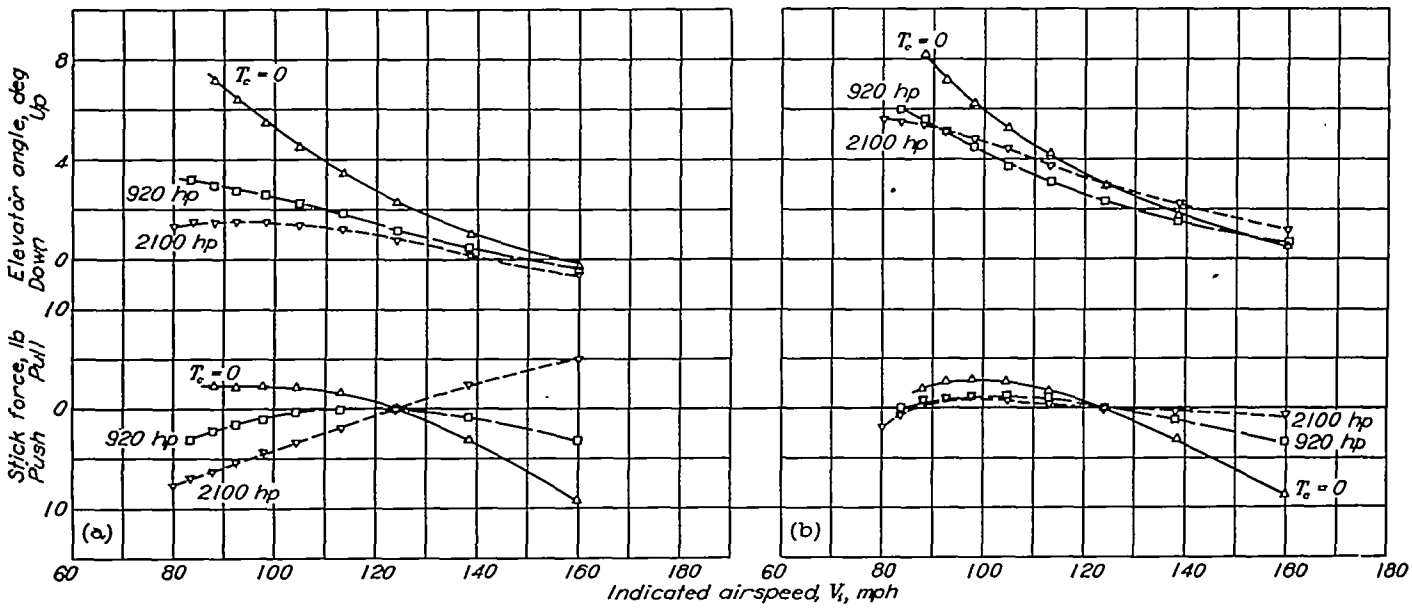

(a) Tilt of the propeller axis = −.8° *c.g.* at .25 M.A.C.

(b) Tilt of the propeller axis = −5.5° *c.g.* at .25 M.A.C.

FIGURE 27.—Effect of propeller operation on longitudinal handling characteristics of a single-engine airplane with two tilts of the propeller axis. Steady flight, normal tail position, common flaps deflected 38°.

TABLE I.—COMPUTATION OF CHANGE IN PITCHING MOMENT DUE TO DIRECT PROPELLER FORCES

[Flight Condition: 2,100 horsepower, Flaps Up]

Constants:

$\frac{2D^2}{S}=\frac{(2)(12.67)^2}{375}=0.855$

$\frac{d(\Delta\alpha)_{power\ on}}{dC_L}=2.18$

$\frac{Z_{-4.8}}{c}-\frac{Z_{-0.8}}{c}=\frac{-1.124}{8.677}-\frac{-0.164}{8.667}=-0.111$

$\frac{l_1}{c}=\frac{11.7}{8.677}=1.355$

1	2	3	4	5	6	7	8	9	10	11	12	13	14	15	16
α	C_L Estimated, or obtained from force test	T_c From T_c against C_L relationship. (See fig. 8.)	$\Delta\left(\Delta C_{m_{\substack{prop.\\thrust}}}\right)=T_c\left(\frac{2D^2}{S}\right)\left(\frac{Z_{-4.8}}{c}-\frac{Z_{-0.8}}{c}\right)$	$\frac{V}{nD}$ From T_c against V/nD characteristics of propeller (see fig. 6). Value used should be that of wind-tunnel test (constant β) or flight (constant C_p) dependent on result desired.	$\left(\frac{V}{nD}\right)^2$	K From K against V/nD characteristics of propeller (see fig. 7). Value used should be that of wind-tunnel test (constant β) or flight (constant C_p) dependent on result desired.	$\Delta\alpha_{power\ on}=\frac{d(\Delta\alpha)_{power\ on}}{dC_L}C_L$	$1+a=\frac{1+\sqrt{1+8/\pi T_c}}{2}$	$\Delta\alpha_{power\ on}=\left(\frac{1}{1+a}\right)(\Delta\alpha_{power\ on})$	$\theta_{-4.8}=\alpha+\Delta\alpha_{power\ on}+$prop. tilt$_{-4.8}$	$\sin\theta_{-4.8}$	$\theta_{-0.8}=\alpha+\Delta\alpha_{power\ on}+$prop. tilt$_{-0.8}$	$\sin\theta_{-0.8}$	$\Delta\left(\Delta C_{m_{\substack{prop.\\normal\\force}}}\right)=\left(\frac{2D^2}{S}\right)\left(\frac{l_1}{c}\right)\left(\frac{K\sin\theta_{-4.8}}{(V/nD)^2}-\frac{K\sin\theta_{-0.8}}{(V/nD)^2}\right)$	$\Delta\left(\Delta C_{m_{prop.}}\right)=\Delta\left(\Delta C_{m_{\substack{prop.\\thrust}}}\right)+\Delta\left(\Delta C_{m_{\substack{prop.\\normal\\force}}}\right)$
−2	0.104	0.015	−0.0015	0.984	0.968	0.082	0.226	1.010	0.224	−7.276	−0.1266	−2.576	−0.0449	−0.0080	−0.0095
0	.276	.064	−.0061	.875	.766	.056	.601	1.039	.579	−4.921	−.0858	−.221	−.0039	−.0069	−.0130
2	.450	.128	−.0122	.769	.591	.039	.980	1.076	.910	−2.590	−.0452	2.110	.0368	−.0063	−.0185
4	.631	.196	−.0185	.690	.476	.032	1.352	1.112	1.216	−.284	−.0050	4.416	.0770	−.0064	−.0249
6	.800	.271	−.0256	.620	.384	.027	1.742	1.150	1.515	2.015	.0352	6.715	.1169	−.0066	−.0322
8	.969	.343	−.0326	.571	.326	.025	2.110	1.185	1.781	4.281	.0746	8.981	.1561	−.0072	−.0398
10	1.129	.413	−.0392	.535	.286	.025	2.458	1.216	2.020	6.520	.1135	11.220	.1946	−.0082	−.0474
12	1.284	.480	−.0455	.505	.278	.024	2.796	1.247	2.241	8.741	.1520	13.441	.2325	−.0081	−.0536
14	1.420	.540	−.0511	.484	.234	.024	3.092	1.271	2.430	10.930	.1896	15.630	.2694	−.0095	−.0606

Plot of the result $\Delta(\Delta C_{m_{prop.}})$ against C_L is given in figure 29 (b).

propeller (referred to hereafter as $\Delta(\Delta C_{m_{prop}})$), is to be evaluated. This eliminates any large discrepancy in the absolute magnitude of $\Delta C_{m_{prop}}$ which might exist. Thus the effect of the tilt of the propeller in the case at hand will be as follows:

$$\Delta(\Delta C_{m_{prop}}) = T_c\left(\frac{2D^2}{S}\right)\left(\frac{z_{-5.5}}{c}-\frac{z_{-0.8}}{c}\right)+ \frac{2D^2}{S}\frac{l_1}{c}\left(\frac{K\sin\theta_{-5.5}}{(V/nD)^2}-\frac{K\sin\theta_{-0.8}}{(V/nD)^2}\right) \quad (6)$$

By use of the above equation and the data of figures 6, 7, 8, and 28, the effect of the direct propeller forces was computed for the several power conditions, flaps up and flaps down. (Table I shows a sample computation for the 2,100-horsepower, flaps up condition and serves as an illustrative example of the method.) The results and the corresponding experimental data obtained from the tail-off runs are shown on figures 29 and 30.

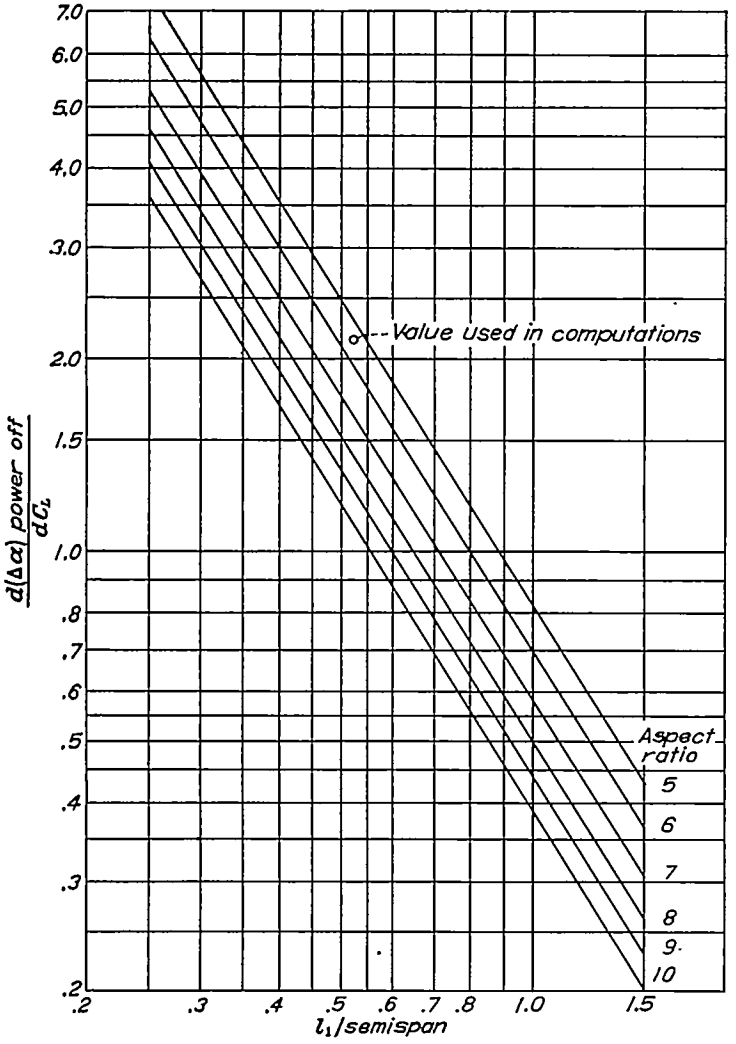

FIGURE 28.—Variation of upwash with distance ahead of 1/4 chord line of elliptic wings of various aspect ratios.

The comparison, both with flaps up and flaps down, is good when considered on the basis of $\Delta(\Delta C_{m_{prop}})$. It is worthy of note that the vertical force contribution to $\Delta(\Delta C_{m_{prop}})$ consists almost entirely of a shift in the curve and contributes very little change in slope. This suggests a considerable simplification of the computation by considering only the T_c term in the above expression for $\Delta(\Delta C_{m_{prop}})$, since normally only the change in slope is of significance, the vertical shift of the curves being unimportant. If this is done and equation (6) is differentiated, considering the second term a constant, the following relationship results:

$$\frac{d\Delta(\Delta C_{m_p})}{dC_L} = \frac{dT_c}{dC_L}\left(\frac{2D^2}{S}\right)\left(\frac{z_{-5.5}}{c}-\frac{z_{-0.8}}{c}\right) \quad (6a)$$

This equation is readily evaluated since for a given tilt of the propeller dT_c/dC_L is the only variable with C_L.

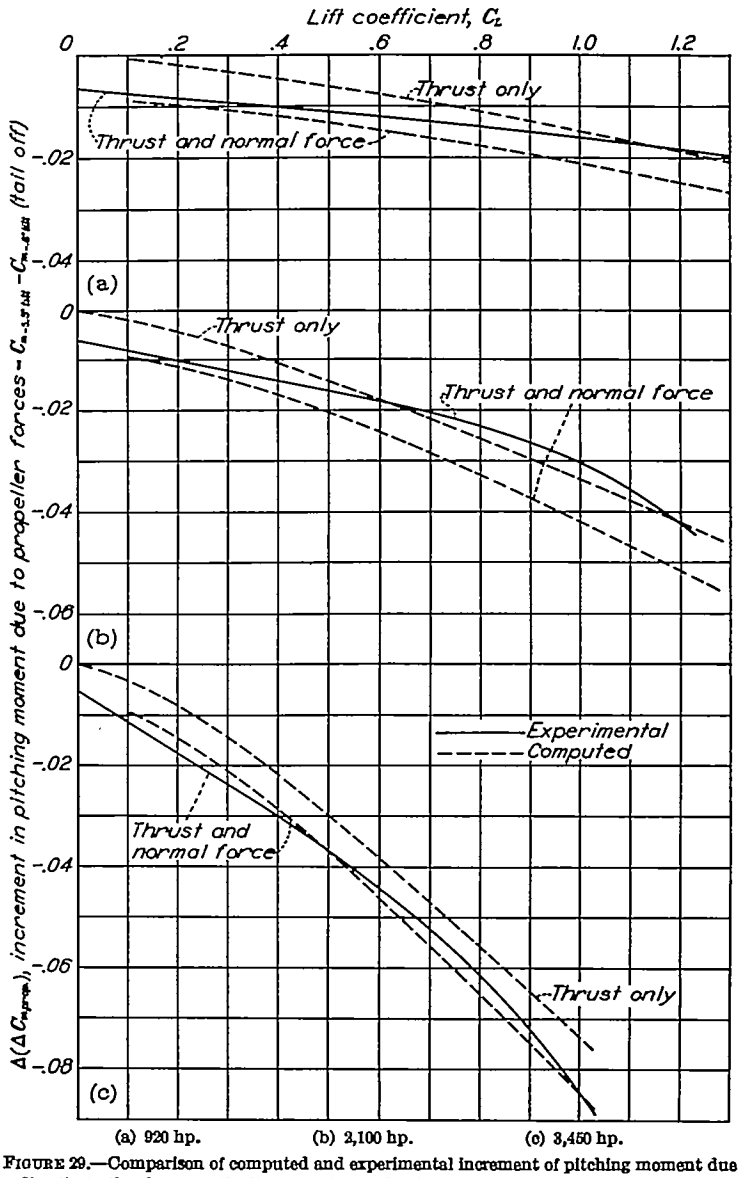

FIGURE 29.—Comparison of computed and experimental increment of pitching moment due directly to the change of the line of action of the thrust and normal force of the tilted propeller. Flaps up.

EFFECT ON THE TAIL PITCHING MOMENT

In accordance with the procedure of reference 1 (and with the simplifying assumption that q/q_0 at the tail with power off is equal to 1), the effect of slipstream on the tail pitching moment can be broken down into the following components:

$$\Delta C_{m_{tail}} = \underbrace{-\Delta\epsilon_{p_{eff}} \frac{dC_m}{di_t}}_{\text{Effect due to change of downwash in the slipstream.}} \underbrace{-\left(\frac{\Delta q}{q_0} \times \Delta\epsilon_p\right)_{eff} \frac{dC_m}{di_t}}_{\text{Effect due to combined change in downwash and } q \text{ in the slipstream.}} + \underbrace{\left(\frac{\Delta q}{q_0}\right)_{eff} C_{m_{t_0}}}_{\text{Effect due to changed } q \text{ in the slipstream.}} \quad (7)$$

It is to be anticipated that tilting the propeller axis will affect the first and second terms by virtue of the difference in downwash increment due to power. This difference will arise from the fact that the vertical component of the thrust is decreased, so that from momentum considerations the downwash induced by the propeller will be decreased. This will be a stabilizing effect. In addition, the changed downwash will result in a different juxtaposition between the slipstream and the tail, so that a different area of the tail will be immersed. As a result $(\Delta q/q_0)_{eff}$ will be changed, and the second and third terms of the preceding equation will be affected. This influence will be stabilizing or destabilizing, dependent on the load on the tail and the original location of the tail in the slipstream.

As was the case in considering the direct propeller forces, the absolute magnitude of $\Delta C_{m_{tail}}$ is not of interest for this analysis, merely the difference in this quantity caused by tilting the propeller (referred to hereafter as $\Delta(\Delta C_{m_{tail}})$). However, this difference cannot be directly evaluated as it was for the direct propeller forces, but must be determined by first computing $\Delta C_{m_{tail}}$ for each tilt of the propeller and then getting the difference. The steps involved in computing $\Delta C_{m_{tail}}$ are as follows:

1. Determine the change in downwash behind the propeller.
2. Determine the location of the tail in the slipstream and the portion of the tail area immersed.
3. Determine the effective values of $\Delta\epsilon_p$ and $\Delta q/q_0$ for substitution in equation (7).

NOTE.—It should be noted that dC_m/di_t is the power-off value measured at an angle of attack where the tail is free of wake effects. This is normally the highest dC_m/di_t measured throughout the angle-of-attack range. In contrast $C_{m_{t_0}}$ is the actual pitching-moment contribution of the tail, power off, that is, the difference between the tail-on and tail-off pitching moment at each angle of attack.

Normal deviations from the assumption of free-stream dynamic pressure at the tail with power off will not cause significant differences in $\Delta C_{m_{tail}}$ as determined from equation (7). If an abnormally large decrease in dynamic pressure exists, the factor $(q/q_0)_{power\ off}$ should be inserted in the first term of equation (7) and $(q_0/q)_{power\ off}$ in the last term.

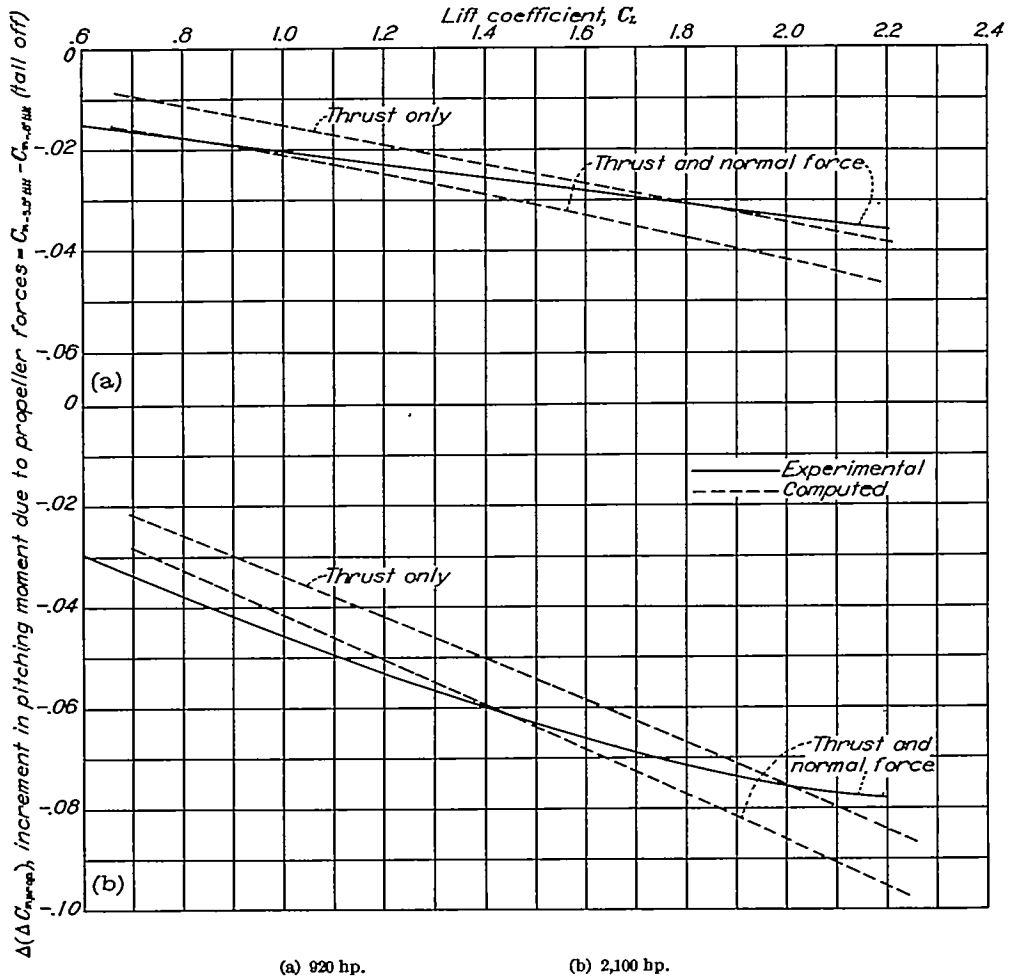

(a) 920 hp. (b) 2,100 hp.

FIGURE 30.—Comparison of computed and experimental increment of pitching moment due directly to the change of the line of action of the thrust and normal force of the tilted propeller. Flaps 38°.

The foregoing procedure must be repeated for the two tilts of the propeller under consideration. The difference in $\Delta C_{m_{tail}}$ computed thereby will be the effect of tilt of the propeller.

The change in downwash is computed by the method of Glauert (pp. 357 to 359, reference 2) with an added term to take care of the fact that θ does not equal α_T (fig. 31) as it does in Glauert's original analysis. (See appendixes B and C.) Thus,

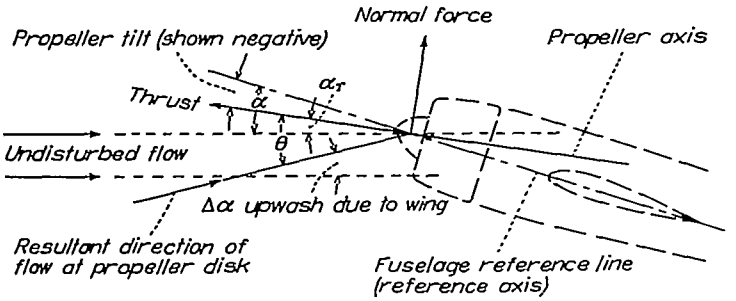

$\alpha_T = \alpha$ + propeller tilt

$\theta = \alpha_T + \Delta\alpha$

$= \alpha$ + propeller tilt + $\Delta\alpha$

FIGURE 31.—Schematic diagram showing definition of angles at propeller.

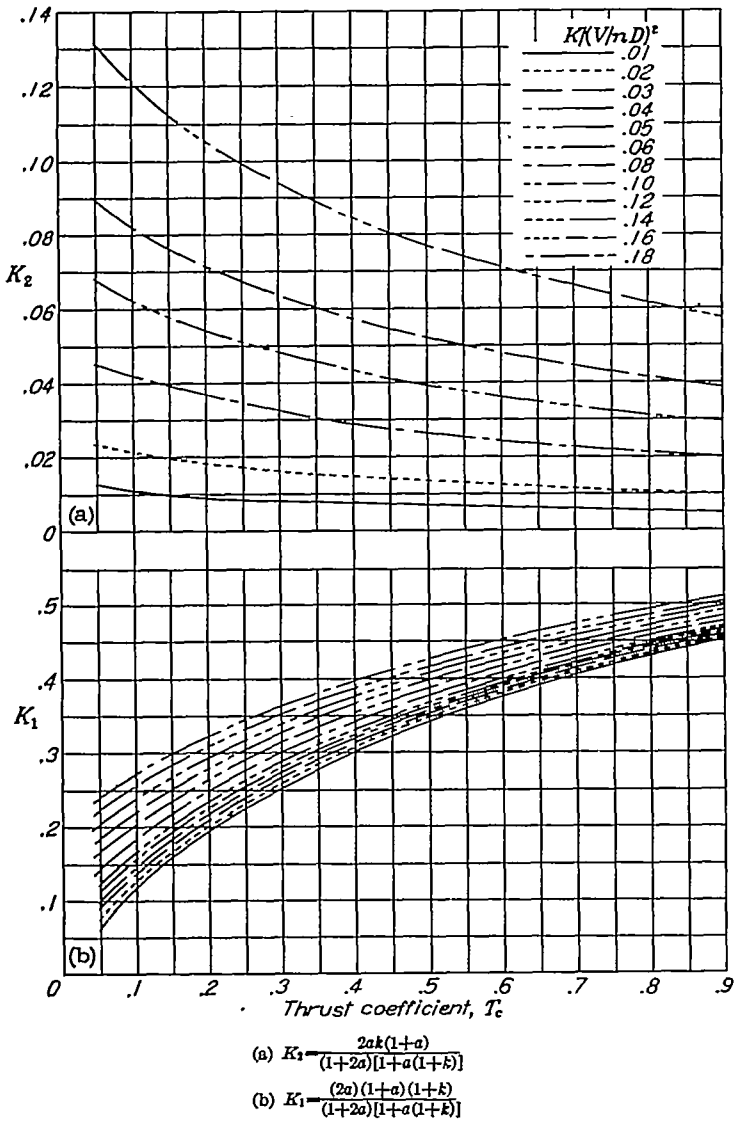

(a) $K_2 = \frac{2ak(1+a)}{(1+2a)[1+a(1+k)]}$

(b) $K_1 = \frac{(2a)(1+a)(1+k)}{(1+2a)[1+a(1+k)]}$

FIGURE 32.—Variation of K_1 and K_2 with T_c and $K/(V/nD)^2$.

$$\Delta\epsilon_p = K_1\alpha_T + K_2\Delta\alpha_{power\ on} \tag{8}$$

$$K_1 = \frac{(2a)(1+a)(1+k)}{(1+2a)[1+a(1+K)]} \tag{9}$$

$$K_2 = \frac{2ak(1+a)}{(1+2a)[1+a(1+k)]} \tag{10}$$

where K is the function of V/nD and blade angle for an inclined propeller used previously for determining the normal force acting on the propeller, and is defined as

$$K = 0.365C_p(V/nD)\left(1 - \frac{V}{nD}\frac{1}{2C_p}\frac{dC_p}{d(V/nD)}\right) \tag{11}$$

The variation of K_1 and K_2 with T_c and $K/(V/nD)^2$ is shown on figure 32.

With the value of $\Delta\epsilon_p$ determined, the location of the slipstream and the area of the tail immersed therein can be determined either graphically or analytically from the geometrical considerations outlined in figure 33.[2]

In accordance with Smelt and Davies (reference 6) the values of $\Delta\epsilon_p$ and $\Delta q/q_0$ are as follows:

$$\Delta\epsilon_{p_{eff}} = 0.6\frac{S_{t_{immersed}}}{S_{tail}}(\Delta\epsilon_p) \tag{12}$$

$$\frac{\Delta q}{q_{0\ eff}} = \lambda\left(\frac{S_{t_{immersed}}}{S_{tail}}\right)s \tag{13}$$

$$\left(\frac{\Delta q}{q_0}\times\Delta\epsilon_p\right)_{eff} = \lambda s(0.6\Delta\epsilon_p)\left(\frac{S_{t_{immersed}}}{S_{tail}}\right) \tag{13a}$$

where

$$s = -1 + \sqrt{1 + \frac{8T_c}{\pi}} \tag{14}$$

and λ is an empirical factor which for usual relations of slipstream and immersed tail will be 1.

Substitution of the appropriate values of $\Delta\epsilon_{p_{eff}}$, $\left(\frac{\Delta q}{q_0}\right)_{p_{eff}}$ and $\left(\frac{\Delta q}{q_0}\times\Delta\epsilon_p\right)_{eff}$ in equation (7) then results in ΔCm_{tail}. It should be observed that dC_m/di_t and Cm_{t_0} are the values estimated, or determined from power-off tests.

The foregoing procedure has been carried out for four tail heights, for both propeller tilts, and the value of $\Delta(\Delta Cm_{tail})$ then determined. (An illustrative computation for the flaps-up, 2,100-horsepower conditions is given in table II.)

The tail heights are 0, 2.25 (normal tail position), 4.50 (raised tail position), and 6.75 feet above the reference line which covers the range likely to be found in normal designs. In terms of the propeller dimensions the heights are approxi-

[2] This procedure is based on the assumptions outlined in reference 1, that the slipstream remains substantially cylindrical. Despite the distortion of the slipstream which is known to exist, the airplanes of reference 1, and at least five other airplanes to which the method has been applied, show that the average $\Delta\epsilon_p$ and the $\Delta q/q_0$ in the slipstream computed from such assumptions correspond quite well with experimental observations. It is true that there is a further change in downwash induced by the propeller in the flow outside the slipstream. This change arises from the changed vortex system of the wing in the slipstream flow. (See Koning, p. 411, reference 2.) If absolute magnitudes of $\Delta C_{m_{tail}}$ were of interest this downwash would have to be evaluated. However, since only the difference in $\Delta C_{m_{tail}}$ due to tilt of the propeller is concerned, only the difference in $\Delta\epsilon_p$ due to the propeller need be evaluated. On the assumption that tilting the propeller will not appreciably affect the wing vortex system, the difference due to tilt of the propeller will consist entirely of that arising from the reduced vertical component of the thrust. This quantity is evaluated by equation (8).

TABLE II.—COMPUTATION OF PITCHING MOMENT OF TAIL (NORMAL POSITION)

[Flight Condition: 2,100 Horsepower, Flaps Up]

Constants: Same as table I plus the following: S_t=85.3 feet; dC_m/di_t=−0.030, λ=1 d_t=2.25 feet

Part 1—Propeller tilt −0.8

1	2	3	4	5	6	7	8	9	10	11	12	13	14	15	16	17	18	19	20	21	22	23	24	25	26	27	28	29	30	31
α	C_L	T_c	From T_c against V/nD charac. of prop. (see fig. 6). Value used should be that of wind-tunnel test (constant β) or flight (constant Cp) dependent on result desired	$\left(\frac{V}{nD}\right)^2$	From K against V/nD charac. of prop. (see fig. 7). Value used should be that of wind-tunnel test (constant β) or flight (constant Cp) dependent on result desired	$\Delta\epsilon_{power\ on}$	$\alpha_T=\alpha+$propeller tilt	$\frac{K}{(V/nD)^2}$	K_1 Propeller downwash factor for values of T_c and V/nD, from figure 32	$\Delta\epsilon_{T_1}=K_1\alpha_T$ Portion of propeller downwash due to α_T	K_2 Propeller downwash factor for values of T_c and V/nD, from figure 33	$\Delta\epsilon_{T_2}=K_2\Delta\epsilon_{power\ on}$	$\Delta\epsilon_T=\Delta\epsilon_{T_1}+\Delta\epsilon_{T_2}$ Total propeller downwash	$\alpha-\Delta\epsilon_T$ Angular difference between slipstream path and reference line (from prop. to wing)	$\frac{l_t(\alpha-\Delta\epsilon_T)}{57.3}$ Displacement (at wing quarter chord) of slipstream center line from reference line	ϵ_{w_0} Downwash behind wing at center line of wake with power off (from reference 7)	$\alpha-\epsilon_{w_0}-\Delta\epsilon_T$ Angular difference between slipstream path and reference line (from wing to tail)	$\frac{l_t(\alpha-\epsilon_{w_0}-\Delta\epsilon_T)}{57.3}$ Displacement (between wing and tail) of slipstream from reference line	$h_t=\frac{l_t(\alpha-\Delta\epsilon_T)}{57.3}+\frac{l_t(\alpha-\epsilon_{w_0}-\Delta\epsilon_T)}{57.3}$ Distance from elevator hinge line to d_t center line of slipstream	b_{l_t} Span of tail intercepted by slipstream (See fig. 33)	c_{l_t} Average chord of tail intercepted by slipstream	$\frac{b_{l_t}c_{l_t}}{S_t}$ Fraction of tail immersed in slipstream	$\Delta C_{m_{t_{due\ to\ prop.\ downwash}}}=-0.6\Delta\epsilon_T\left(\frac{b_{l_t}c_{l_t}}{S_t}\right)\frac{dC_m}{di_t}$	$\epsilon=-1+\sqrt{1+8/\pi\ T_c}$ Increment of velocity in slipstream	$\Delta C_{m_{t_{due\ to\ prop.\ downwash\ and\ \Delta q/q_0}}}=-0.6\left(0.6\Delta\epsilon_T\frac{b_{l_t}c_{l_t}}{S_t}\right)\frac{dC_m}{di_t}$	$\Delta C_{m_{t_0}}$ Tail pitching moment, power off. Estimated or taken from power-off wind-tunnel tests	$\Delta C_{m_{t_{due\ to\ \Delta q/q_0}}}=\lambda^2\left(\frac{b_{l_t}c_{l_t}}{S_t}\right)C_{m_{q_0}}$	Total $\Delta C_{m_{T-0.8}}$=column 24+column 26+column 28	Total $\Delta=C_{T-0.8}$ From column 29 in part 2 of table	This result is plotted $\Delta(\Delta C_{m_{tail}})=\Delta C_{m_{T-0.8}}-\Delta C_{m_{T-5.5}}$ against C_L on figure 34
															These steps can be performed graphically as shown in figure 36															
−2	.074	.011		.995	.990	.086	.22	−2.8	.087	.105	−.29	.02	−.27	−1.73	−.353	.55	−2.28	−.895	−3.50	10.51	5.09	.620	−.0030	.015	0	.120	.0011	−.0019	.0078	−.0059
0	.258	.058		.886	.785	.059	.58	−1.8	.075	.142	−.11	.032	−.06	−1.06	−.012	1.92	−1.86	−.731	−2.97	11.16	5.04	.660	−.0010	.073	−.0001	.092	.0043	.0032	.0051	−.0083
2	.440	.125		.773	.598	.030	.01	1.2	.065	.100	−.23	.065	.29	1.71	.349	3.28	−1.57	−.617	−2.52	11.61	5.01	.630	−.0035	.148	−.0005	.064	.0056	.0096	.0030	−.0126
4	.625	.198		.687	.472	.032	1.52	3.2	.068	.240	−.77	.062	.85	3.15	.043	4.65	−1.50	−.589	−2.20	11.87	4.99	.693	−.0106	.226	−.0024	.034	.0035	.0165	.0007	−.0172
6	.809	.274		.618	.382	.027	1.47	5.2	.071	.283	1.47	.057	1.56	4.44	.906	6.01	−1.57	−.715	−2.90	12.04	4.98	.700	−.0197	.303	−.0060	.004	.0019	.0238	.0019	−.0219
8	.991	.353		.564	.318	.025	2.33	7.2	.079	.323	2.33	.059	2.44	5.56	1.135	7.38	−1.82	−.797	−1.70	12.17	4.97	.706	−.0433	.441	−.0191	.026	.0117	.0309	.0043	−.0206
10	1.157	.425		.529	.280	.025	3.28	9.2	.089	.356	4.20	.063	3.41	6.59	1.346	8.62	−2.03	−.868	−1.57	12.23	4.96	.709	−.0565	.500	−.0283	.055	.0246	.0378	.0069	−.0309
12	1.314	.493		.501	.251	.024	4.20	11.2	.096	.383	5.31	.062	4.43	7.57	1.545	9.78	−2.21	−.856	−1.36	12.33	4.95	.715	−.0703	.547	−.0385	.082	.0388	.0460	.0114	−.0346
14	1.430	.548		.481	.231	.023	5.46	13.2	.100	.402	6.31	.062	.15	8.54	1.744	10.72	−2.18									.108	.0553	.0535	.0142	−.0393

Part 2—Propeller tilt −5.5

α	C_L	T_c	$\frac{V}{nD}$	$\left(\frac{V}{nD}\right)^2$	K	$\Delta\epsilon_{power\ on}$	α_T	$\frac{K}{(V/nD)^2}$	K_1	$\Delta\epsilon_{T_1}$	K_2	$\Delta\epsilon_{T_2}$	$\Delta\epsilon_T$	$\alpha-\Delta\epsilon_T$	$\frac{l_t(\alpha-\Delta\epsilon_T)}{57.3}$	ϵ_{w_0}	$\alpha-\epsilon_{w_0}-\Delta\epsilon_T$	$\frac{l_t(\alpha-\epsilon_{w_0}-\Delta\epsilon_T)}{57.3}$	h_t	b_{l_t}	c_{l_t}	$\frac{b_{l_t}c_{l_t}}{S_t}$	$\Delta C_{m_{t_{due\ to\ prop.\ downwash}}}$	ϵ	$\Delta C_{m_{t_{due\ to\ prop.\ downwash\ and\ \Delta q/q_0}}}$	$\Delta C_{m_{t_0}}$	$\Delta C_{m_{t_{due\ to\ \Delta q/q_0}}}$	Total $\Delta C_{m_{T-5.5}}$		
−2	Same as for −0.8 tilt		Same as for −0.8 tilt																											
0																														
2																														
4																														
6																														
8																														
10																														
12																														
14																														

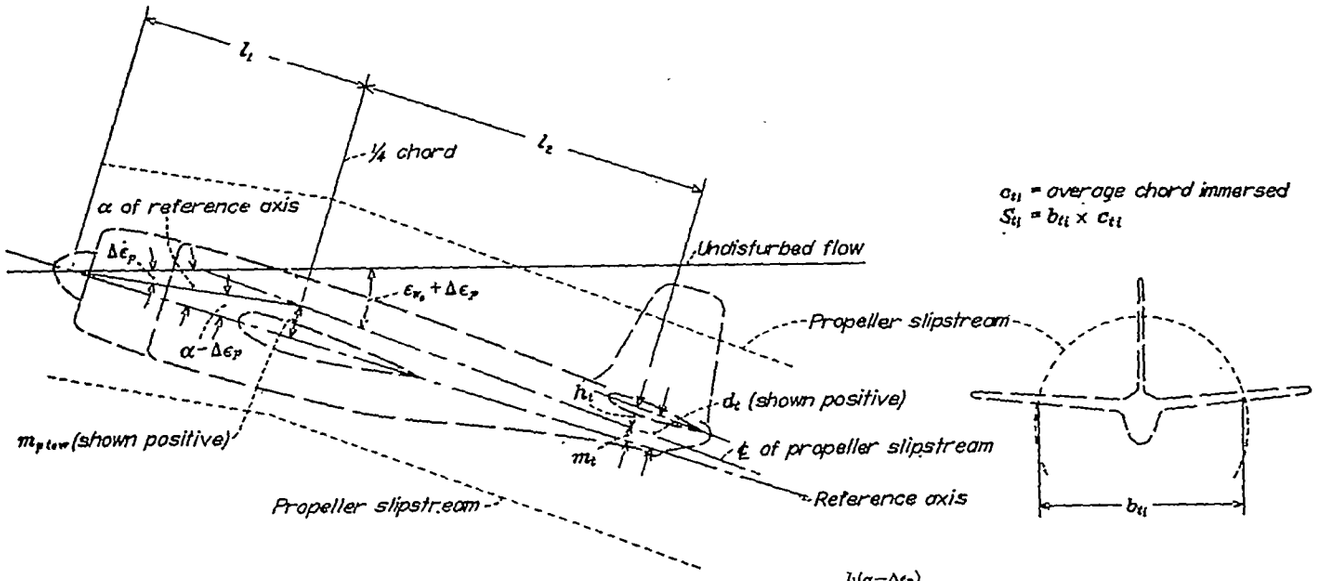

Slipstream displacement from propeller to wing $= m_{p\,to\,w} = \frac{l_1(\alpha-\Delta\epsilon_p)}{57.3}$

Slipstream displacement from wing to tail $= m_{w\,to\,t} = \frac{l_2(\alpha-\epsilon_{w_0}-\Delta\epsilon_p)}{57.3}$

Slipstream displacement at tail $= m_t = m_{p\,to\,w} + m_{w\,to\,t}$

Height of tail above slipstream $h_t = m_t - d_t$

FIGURE 33.—Graphical illustration of relation between tail location and center line of slip-stream.

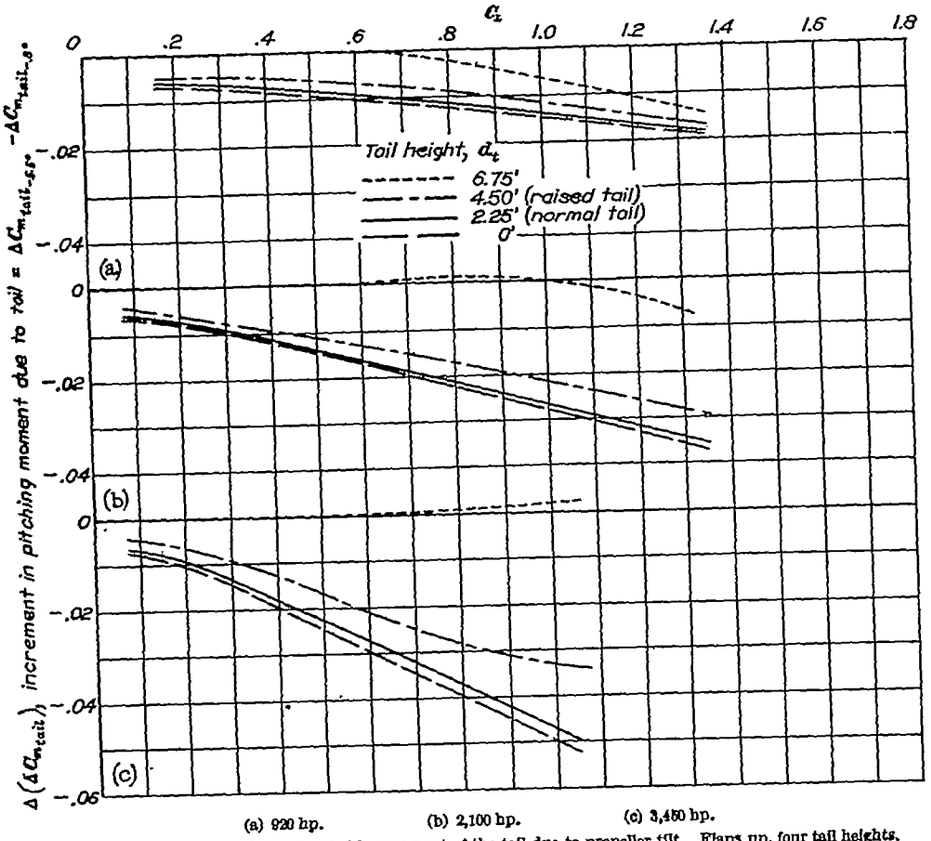

(a) 920 hp. (b) 2,100 hp. (c) 3,450 hp.

FIGURE 34.—Computed change in pitching moment of the tail due to propeller tilt. Flaps up, four tail heights.

mately 0, $1/3R$, $2/3R$, and R above the reference line. The computed values of $\Delta(\Delta C_{m_{tail}})$ are shown on figures 34 and 35. They furnish an idea of the magnitude of the effects of tilt of the propeller on the tail, and the rate at which these effects change with tail height. It will be observed that, with flaps up, the normal tail is in the position which experiences close to the maximum effect, amounting to a change in dC_m/dC_L of -0.022 at a C_L of 0.8 (compared to -0.046 obtained from the direct propeller forces). The higher tail positions are farther from the center of the slipstream and, therefore, less affected by it. To give a physical picture of this effect, and to clarify the steps of the computation, figures 36 and 37 have been prepared showing the relative location of the tail and slipstream, the tail area immersed and the magnitude of the $\Delta\epsilon_p$ and $\Delta q/q_0$ effect. As shown on figure 37, with flaps down, the slipstream is below the tail for the major part of the operating range and, therefore, $\Delta(\Delta C_{m_{tail}})$ is zero. Reference to these two figures will aid in following the computation outline of tables I and II.

The extent to which the experiment confirms the computations is shown on figures 38 and 39, where the summation of the computed effect of the direct propeller forces and the tail effects is compared with the experimental determination. For the flaps-up condition, where a major portion of the tail is immersed in the slipstream, the computations tend to overestimate the effect of the tilt of the propeller on the tail. This is probably due to the slipstream being distorted rather than the idealized cylindrical shape. The fact that some small effect is measured flaps down, when the computations indicate the tail to be just out of the slipstream, fits in with the hypothesis. It is worthy of note that the theory indicates the proper trend; that is, the reduced effect of tilt on the raised tail, which was measured (fig. 15), is predicted (fig. 34).

The over-all accuracy of the method can be judged on the basis of figures 38 and 39. At the higher powers (where the effects of experimental scatter are less pronounced) the predicted increment in $\Delta(\Delta C_m)$ tends to run between 1.1 and 1.2 of that measured. It is believed that such a check is close enough to justify use of the method in analyses which are made in the preliminary design stage and will serve to evaluate with sufficient accuracy the benefits to be obtained from tilt of the propeller.

CONCLUDING REMARKS

The experimental results are considered to show quite definitely the advantages to be gained by a downward tilt of the propeller. It is clearly indicated that a 5° downward tilt of the propeller will cause a rearward shift of the neutral point ranging from 0.05 to 0.10 M. A. C. at normal climb lift coefficients with power typical of modern airplanes. This should considerably ease the difficulty of obtaining stability under these high-power low-speed conditions, so that a reduction in the high-speed stability, where power effects are negligible, would be permissible. Advantage can then be taken of this fact in order to ease the elevator balance requirements for the attainment of low stick forces per g.

The generalization of the results is made possible by the use of the computation procedure outlined. It is believed that the check between the over-all experimental and predicted results is sufficiently close to justify use of the method in the preliminary design stage.

AMES AERONAUTICAL LABORATORY,
NATIONAL ADVISORY COMMITTEE FOR AERONAUTICS,
MOFFETT FIELD, CALIF., 1944.

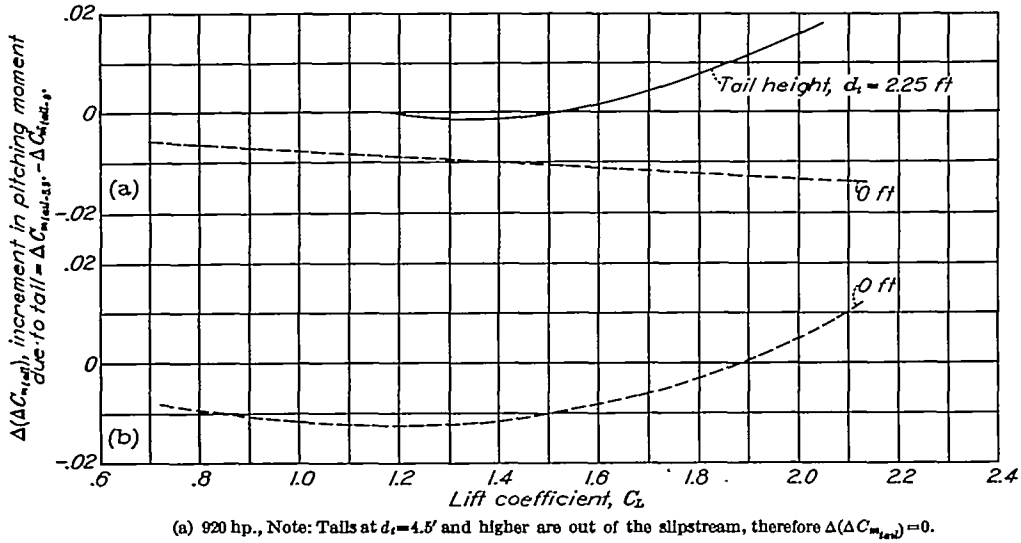

(a) 920 hp., Note: Tails at d_t=4.5′ and higher are out of the slipstream, therefore $\Delta(\Delta C_{m_{tail}})=0$.

(b) 2,100 hp., Note: Tails at d_t=2.25′ and higher are out of the slipstream, therefore $\Delta(\Delta C_{m_{tail}})=0$.

FIGURE 35.—Computed change in pitching moment of the tail due to propeller tilt. Flaps deflected 38°.

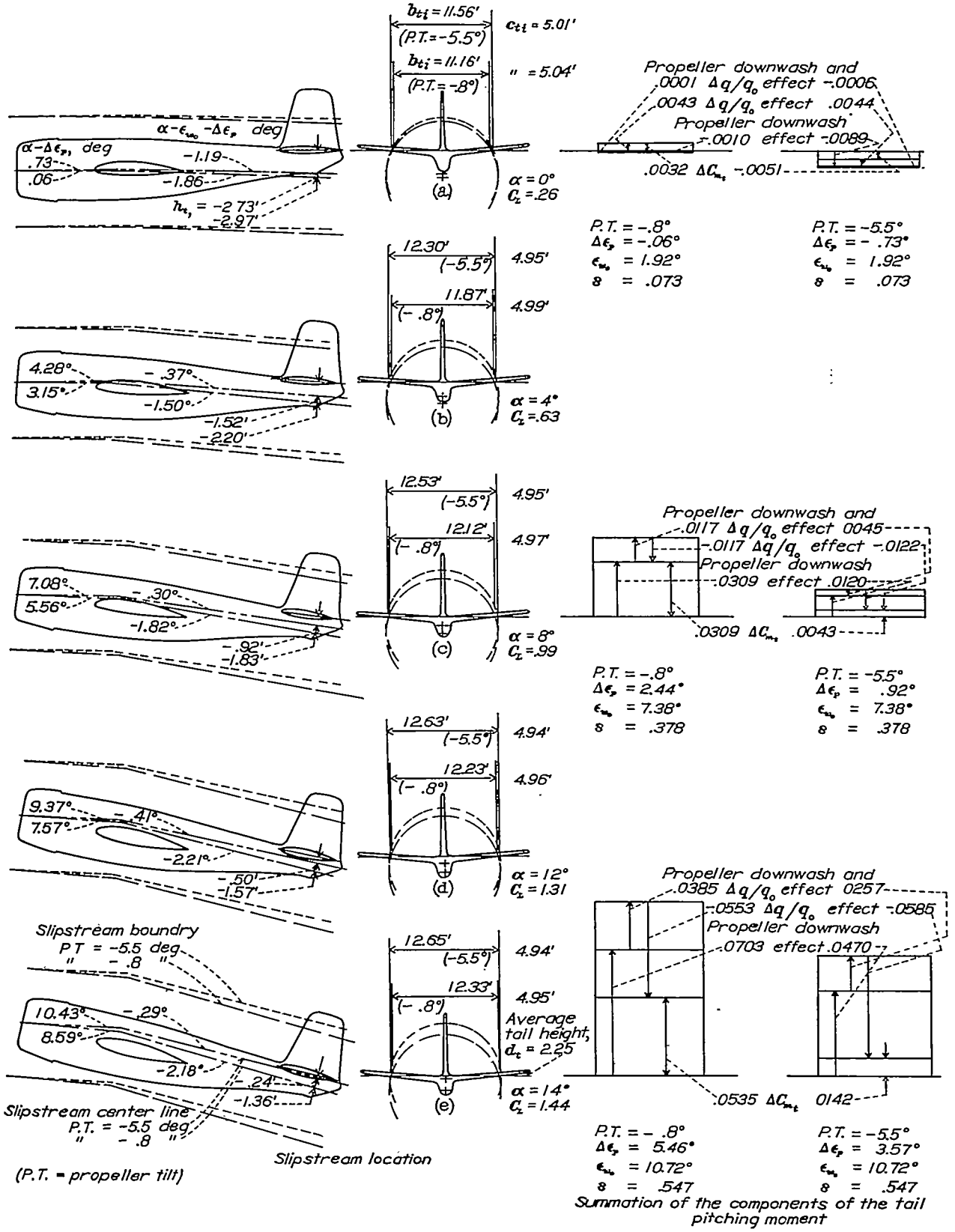

FIGURE 36.—Schematic pictures of slipstream location with two tilts of the propeller axis. Normal tail location, flaps 0°, 2,100 horsepower.

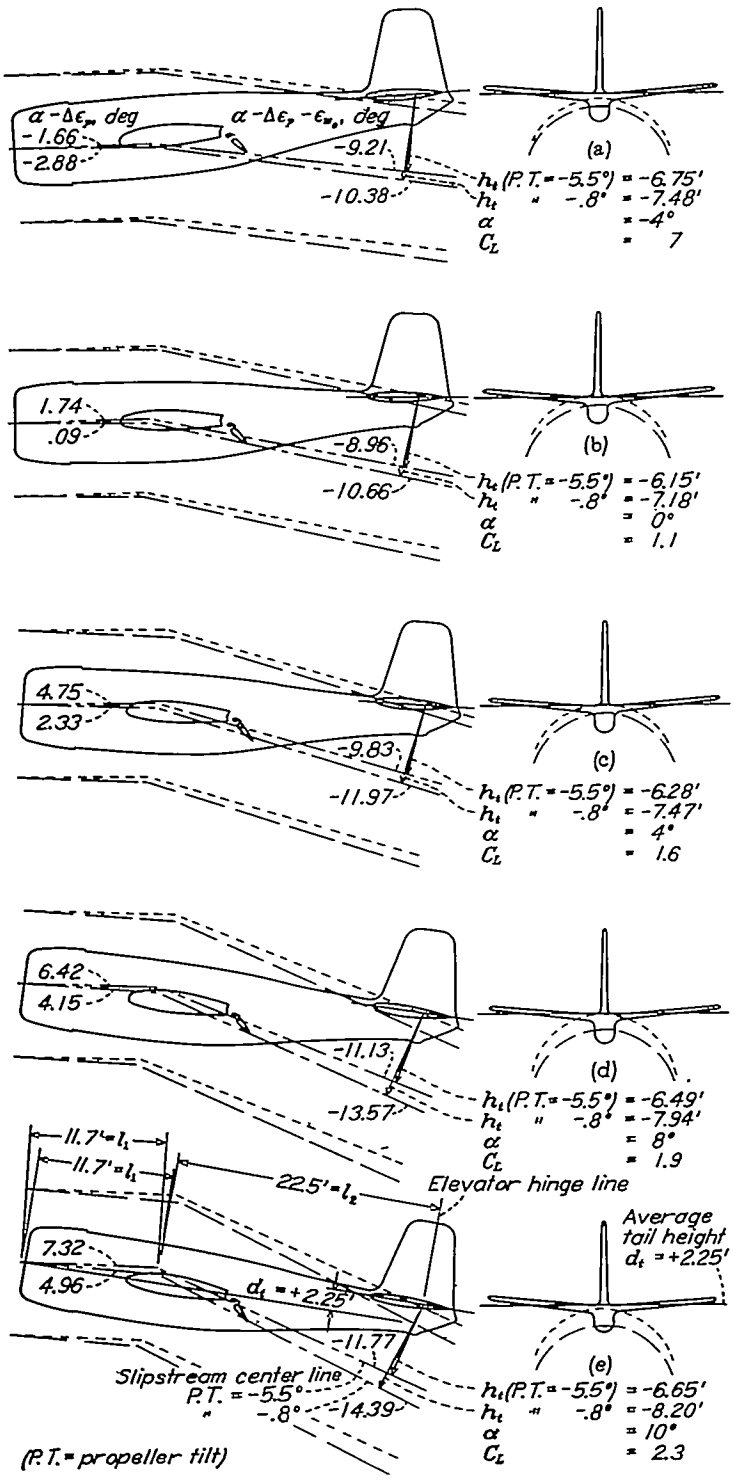

FIGURE 37.—Schematic pictures of slipstream location with two tilts of the propeller axis. Normal tail location, flaps deflected 38°, 2,100 horsepower.

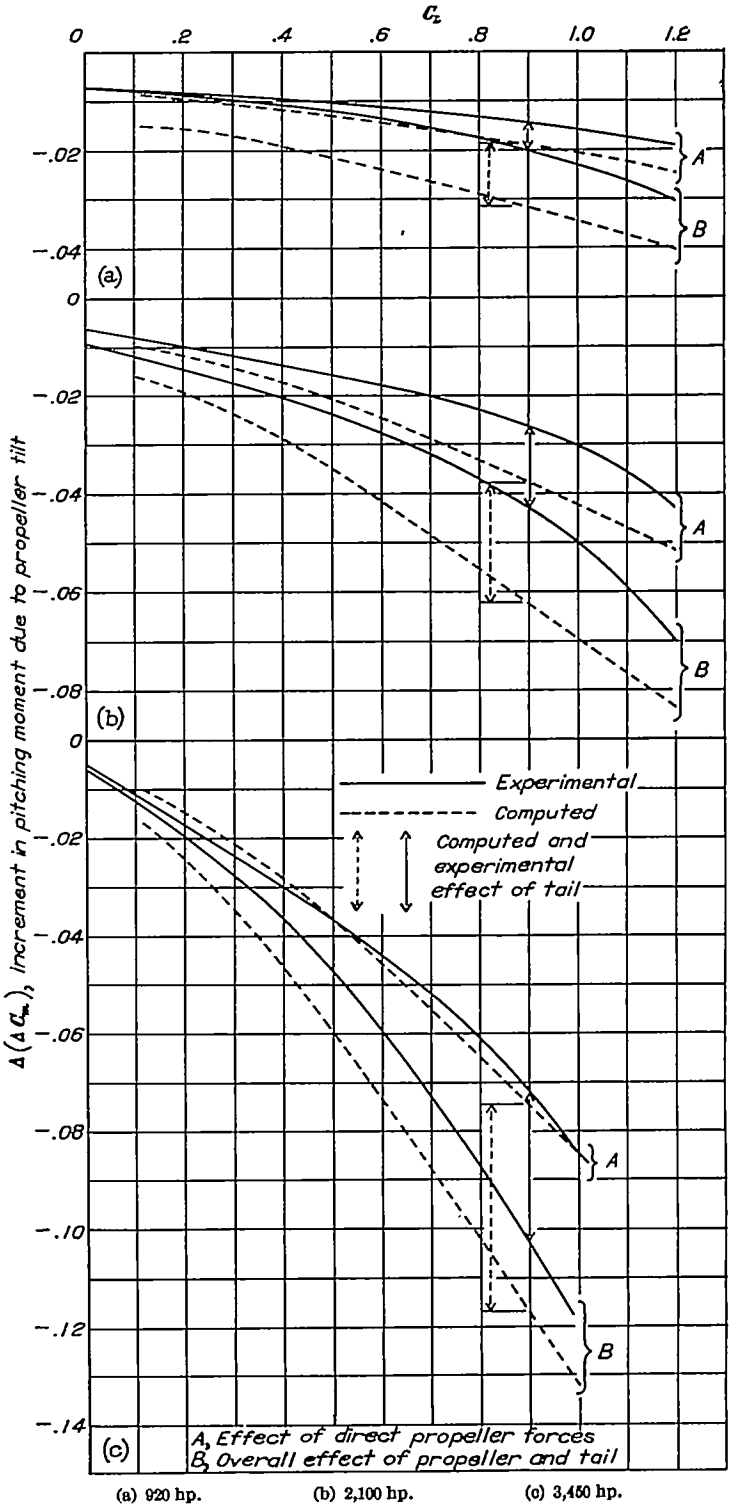

(a) 920 hp. (b) 2,100 hp. (c) 3,450 hp.

FIGURE 38.—Comparison of the over-all computed and experimental effects of propeller tilt. Flaps up, normal tail.

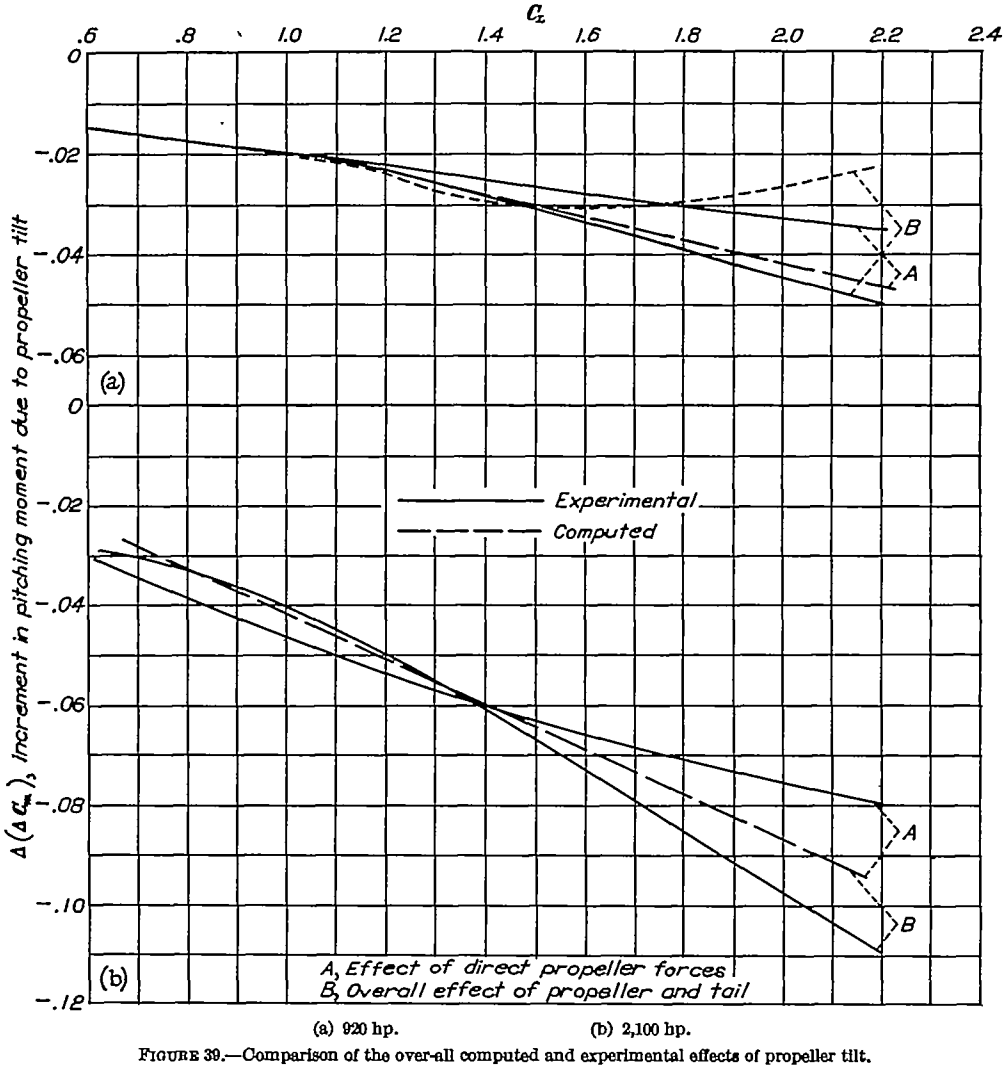

(a) 920 hp. (b) 2,100 hp.

FIGURE 39.—Comparison of the over-all computed and experimental effects of propeller tilt. Flaps deflected 38°, normal tail.

APPENDIX A

SYMBOLS

The following symbols are used in this report. Wherever possible standard symbols have been used.

C_L	Lift coefficient
C_D	Drag coefficient
C_m	Pitching-moment coefficient
$\Delta C_{m_{prop}}$	Change in pitching-moment coefficient due to direct propeller forces
$\Delta C_{m_{tail}}$	Change in pitching-moment coefficient due to slipstream on tail
ΔC_m	Summation of $\Delta C_{m_{prop}}+C_{m_{tail}}$
$\Delta(\Delta C_m)$	Increment in ΔC_m due to propeller tilt
dC_m/di_t	Rate of change of pitching-moment coefficient with tail incidence
$C_{m_{t_0}}$	Pitching moment due to tail, with power off. If power-off force tests are available, this can be determined from difference between C_m with tail on, C_m with tail off, at equal α (not equal C_L)
D	Propeller diameter
R	Propeller radius
V	Airspeed
n	Revolutions of propeller per second
ρ	Air density
P	Power input to propeller
C_p	Power coefficient $\left(\frac{P}{\rho n^3 D^5}\right)$
T	Axial propeller thrust
T_c	Thrust coefficient $\left(\frac{T}{\rho V^2 D^2}\right)$
N_P	Force normal to propeller axis due to inclination of propeller to air stream
C_{N_p}	Propeller normal-force coefficient $\left(\frac{N_P}{\rho n^2 D^4}\right)$
K	Propeller normal-force factor, $0.365 C_p \left(\frac{V}{nD}\right)\left(1-\frac{V}{nD}\frac{1}{2C_p}\frac{dC_p}{d(V/nD)}\right)$ (See fig. 7 for variation of K against V/nD for test propeller at $\beta=21.0^0$.)
K_1	Parameter for determining downwash behind inclined propeller due to α_T
K_2	Parameter for determining downwash behind inclined propeller due to $\Delta\alpha$
k	Factor used in computing K_1 and K_2 $\left(\frac{K/(V/nD)^2}{T_c}\right)$
α	Angle of reference axis to relative wind
α_T	Angle of propeller thrust axis to relative wind, α+tilt of the propeller
$\Delta\alpha_{power\ off}$	Wing upwash at propeller disk without slipstream inflow (upflow positive)
$\Delta\alpha_{power\ on}$	Wing upwash at propeller disk with slipstream inflow
θ	Inclination of propeller axis to resultant direction of wind at horizontal center line of propeller disk ($\alpha_T+\Delta\alpha$)
$d\theta/d\alpha$	Ratio of rate of change of θ to α (dependent on distance ahead of wing, fig. 28)
ϵ_{w_0}	Downwash behind wing, with power off (to be taken as that at center line of wake unless slipstream is very much above or below wing)
$\Delta\epsilon_p$	Increment in downwash, in slipstream due to propeller forces
$\Delta\epsilon_{p_1}$	That part of $\Delta\epsilon_p$ due to α_T
$\Delta\epsilon_{p_2}$	That part of $\Delta\epsilon_p$ due to $\Delta\alpha$
q	Local dynamic pressure
q_o	Free-stream dynamic pressure
Δq	$(q-q_o)$ in slipstream
$(\Delta\epsilon_p)_{eff}$	Effective change in these two quantities as determined by change in tail pitching moment
$(\Delta q/q_o)_{eff}$	
a	Velocity increment factor at propeller disk
$V(1+a)$	Air velocity through propeller
s	Velocity increment factor back of propeller disk $\left(-1+\sqrt{1+\frac{8T_c}{\pi}}\right)$
$V(1+s)$	Air velocity back of propeller disk in the slipstream
S	Wing area
S_t	Tail area
S_e	Elevator area aft of hinge line
b	Wing span
b_{t_t}	Span of tail immersed in slipstream
c	Wing mean aerodynamic chord
c_{t_t}	Average chord of tail immersed
S_{t_t}	Area of tail immersed in slipstream $(b_{t_t}\times c_{t_t})$
$\overline{c_e}$	Average elevator chord aft of hinge line
i_t	Tail incidence to reference line
δ_e	Elevator angle, degrees
l_1	Distance from propeller disk to center of gravity of airplane (measured parallel to thrust line)
l_2	Distance from center of gravity to elevator hinge line (measured parallel to thrust line)
z	Distance from center of gravity to thrust line, positive when center of gravity is above thrust line (measured perpendicular to thrust line)
d_t	Distance from elevator hinge line to reference axis, positive when tail is above reference axis (measured perpendicular to reference axis)
h_t	Distance from slipstream center line to tail, positive when slipstream is above tail
H	Elevator hinge moment
C_{h_e}	Elevator hinge-moment coefficient $\left(\frac{H}{qS_e c_e}\right)$
dC_{h_e}/di_t	Rate of change of elevator hinge-moment coefficient with tail incidence
F	Elevator stick force
g	Acceleration of gravity (32.2 ft/sec^2)

Subscripts

-5.5 -0.8	magnitude of tilt of the propeller axis

APPENDIX B

In the computation of the normal force acting on a propeller in the presence of a wing it is necessary to know the additional effective tilt of the propeller ($\Delta\alpha$), caused by the upwash in front of the wing. In the report this has been expressed as

$$\Delta\alpha_{\text{power off}}=\frac{d(\Delta\alpha_{\text{power off}})}{dC_L}\,C_L \tag{B1}$$

$$\Delta\alpha_{\text{power on}}=\left(\frac{1}{1+a}\right)(\Delta\alpha_{\text{power off}}) \tag{B2}$$

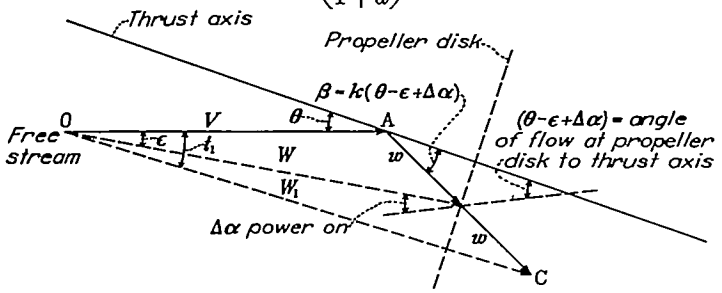

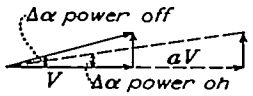

FIGURE 40.—Diagrammatic representation of flow at propeller disk.

The relation between the power-off and the power-on $\Delta\alpha$ takes into account the increased axial velocity at the propeller (fig. 40) due to inflow. The value of $\frac{d(\Delta\alpha_{\text{power off}})}{dC_L}$ is given in figure 28 as a function of the two main variables, wing aspect ratio and distance forward of the wing quarter chord line. (Vertical location of propeller assumed to be sufficiently close to x-axis of wing so that it is not a significant variable.) This variation has been derived as follows. The downwash ϵ at any point along the x-axis of the wing with elliptical span loading will be

$$\epsilon=\frac{2}{\pi}\epsilon_0\int_0^{b/2}\left\{1-\frac{x^2-\eta^2}{x}\right\}\frac{d\eta}{\sqrt{(b/2)^2-\eta^2}} \tag{B3}$$

where

$$\eta=\frac{b}{2}\cos\theta$$

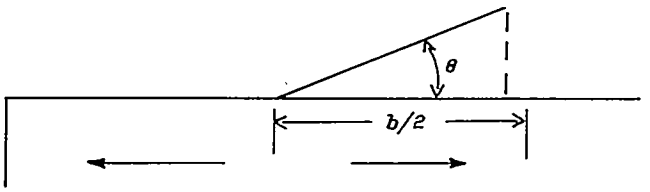

and ϵ_0 is the downwash at the lifting line

$$\epsilon_0=\frac{C_L}{\pi A} \tag{B4}$$

and in the terms of the sign conventions of this report

$$\Delta\alpha=-\epsilon$$

Substituting in equation (B3) and differentiating gives

$$\frac{d(\Delta\alpha)}{dC_L}=-\frac{d\epsilon}{dC_L}=-\frac{2}{\pi^2 A}\int_0^{b/2}\left\{1-\frac{x^2-\eta^2}{x}\right\}\frac{d\eta}{\sqrt{(b/2)^2-\eta^2}} \tag{B5}$$

The curves of figure 28 are a plot of this equation for various values of $\frac{x}{b/2}$ and aspect ratio.

APPENDIX C

In this appendix the symbol notation used by Glauert in reference 2 is used, rather than that of the main body of this report, so that ready cross reference can be made.

Glauert in reference 2 (pp. 357–360) develops a relation between the side force Y on a propeller and the increased angle of downwash ϵ behind it. For the case considered the side force is proportional and

$$Y=\beta T \tag{C1}$$

$$\beta=k(\theta-\epsilon) \tag{C2}$$

where

$$k=\frac{A\lambda Q}{TR}\left[1-\frac{\lambda}{2Q_c}\times\frac{dQ_c}{d\lambda}\right]$$

$$=0.365C_p\left(\frac{V}{nD}\right)\left(1-\frac{V}{nD}\,\frac{1}{2C_p}\times\frac{dC_p}{d(V/nD)}\right)$$

The angle $(\theta-\epsilon)$ as shown in figure 123 of reference 2 is the inclination of the propeller at the propeller disk. In the case of a propeller in the presence of the wing, the inclination of the propeller is increased by $\Delta\alpha$, the upwash in front of the wing at the propeller disk. (See fig. 40 of this report.) Thus for this case

$$\beta=K(\theta-\epsilon+\Delta\alpha) \tag{C3}$$

Substitution of this expression for β (instead of equation (C2)) in the equations

$$\frac{\epsilon}{\theta-\beta}=\frac{w}{V+w}=\frac{a}{1+a} \tag{C4}$$

$$\frac{\epsilon_1}{\theta+\beta}=\frac{2w}{V+2w}=\frac{2a}{1+2a} \tag{C5}$$

results in the following

$$\epsilon=\frac{a(1+k)\theta}{1+a(1+k)}-\frac{\Delta\alpha ka}{(1-a)[1+a(1+k)]} \tag{C6}$$

and

$$\epsilon_1=\left\{\frac{\theta(2a)(1+a)(1+k)}{(1+2a)[1+a(1+k)]}\right\}-\frac{\Delta\alpha 2ak(1+a)}{(1+2a)[1+a(1+k)]} \tag{C7}$$

It will be noted that the first term of each of the above equations is that due to the inclination of the propeller to the free stream and is equal to the Glauert expression for same. The second term is the supplemental downwash arising from the increase in propeller normal force due to the wing upwash.

In the report K_1 and K_2 are defined in accordance with equation (C7) so that

$$\epsilon_1=K_1\theta+K_2\Delta\alpha \tag{C8}$$

The variation of K_1 and K_2 with $K/(V/nD)^2$ and T_c is given in figure 32.

REFERENCES

1. Goett, Harry J., and Pass, H. R.: Effects of Propeller Operation on the Pitching Moments of Single-Engine Monoplanes. NACA ACR, May 1941.
2. Durand, W. F.: Aerodynamic Theory. Vol. IV, Julius Springer (Berlin), 1934.
3. Ribner, Herbert S.: Propellers in Yaw. NACA ARR No. 3L09, 1943.
4. Ribner, Herbert S.: Formulas for Propellers in Yaw and Charts for the Side-Force Derivative. NACA ARR No. 3E19, 1943.
5. Ribner, Herbert S.: Proposal for a Propeller Side-Force Factor NACA RB No. 3L02, 1943.
6. Smelt, R. and Davies, H: Estimation of Increase in Lift Due to Slipstream. R. & M. No. 1788, British A. R. C., 1937.
7. Silverstein, Abe, and Katzoff, S.: Design Charts for Predicting Downwash Angles and Wake Characteristics Behind Plain and Flapped Wings. NACA Rep. No. 648, 1939.